energies

MDPI

Article

Hybrid Operational Strategies for Smart Renewable Energy Deployment in Port Infrastructures Toward Efficiency, Sustainability and Innovation

Toni X. Adrover [1], Aitor Fernandez Jimenez [2], Rodolfo Espina-Valdés [2], Modesto Perez-Sanchez [3,*], Oscar E. Coronado-Hernández [4], Aonghus McNabola [5] and Helena M. Ramos [1,*]

[1] Civil Engineering Research and Innovation for Sustainability (CERIS), Instituto Superior Técnico, Department of Civil Engineering, Architecture and Environment, University of Lisbon, 1049-001 Lisbon, Portugal
[2] Department of Energy, CUIDA, University of Oviedo, 33003 Oviedo, Spain; fernandezaitor@uniovi.es (A.F.J.); espinarodolfo@uniovi.es (R.E.-V.)
[3] Hydraulic Engineering and Environmental Department, Universitat Politècnica de València, 46022 Valencia, Spain
[4] Instituto de Hidráulica y Saneamiento Ambiental, Universidad de Cartagena, Cartagena 130001, Colombia
[5] School of Engineering, RMIT University, 124 La Trobe St, Melbourne, VIC 3000, Australia; aonghus.mcnabola@rmit.edu.au
* Correspondence: mopesan1@upv.es (M.P.-S.); hramos.ist@gmail.com or helena.ramos@tecnico.ulisboa.pt (H.M.R.)

Abstract

This research presents the development of a new Hybrid Operational Strategy model for energy management optimization designed to evaluate the feasibility of implementing hybrid renewable energy modules in ports, aiming to improve their efficiency, sustainability, and innovation. The proposed system integrates photovoltaic, wind, and hydrokinetic energy sources, incorporating electronic components and assessing two energy storage technologies—Pump-as-Turbine (PAT) and battery systems—to determine the most viable solution for practical deployment. The optimization algorithm allows a concurrent refinement process for the power generation data of each renewable source. Four scenarios were analyzed within this optimization framework: two assessing the performance of single modules employing each storage technology individually, and two exploring configurations with multiple modules operating in parallel, either with independent storage units or a single centralized system. Battery storage was identified as the most feasible option based on the optimization outcomes. Considering the demand characteristics and generation capacity of the hybrid module, the configuration yielding the best overall performance consisted of a single module incorporating battery storage, achieving 90% demand coverage and demonstrating economic viability with a Net Present Value (NPV) of 9182.79 € and an Internal Rate of Return (IRR) of 10.88%.

Keywords: hybrid operation strategies; smart renewable energy solutions; energy management; ports' infrastructures; efficiency; sustainability and innovation

Academic Editors: Alexander Micallef and Muhammad Sadiq

Received: 17 December 2025
Revised: 26 January 2026
Accepted: 28 January 2026
Published: 30 January 2026

1. Introduction

Europe is currently undergoing a broad energy transition driven by the increasing adoption of clean energy sources. This shift involves the gradual replacement of conventional fossil-fuel-based generation technologies, such as coal and natural gas, with renewable alternatives. Within this context, the European Union (EU) has introduced

a comprehensive set of initiatives to accelerate decarbonization not only at the macro-system scale but also across residential, industrial, and infrastructural domains, including maritime and port facilities. Port infrastructures, in particular, are recognized as highly energy-intensive nodes within the transport and logistics chain [1], where electrification plays a key role in reducing greenhouse gas emissions. Notably, the FuelEU Maritime Regulation (EU 2023/1805) stipulates that, from 2030 onward, all container and passenger vessels of 5000 gross tonnage or more must be equipped to connect to onshore power supply (OPS) systems while berthed [2]. The implementation of such regulatory measures is expected to substantially increase electricity demand across European ports. Current projections estimate that shore power consumption could range between 6 and 13 TWh per year within the European Union ports [3]. To ensure that this process effectively contributes to emission reduction objectives, the electricity supplied to port facilities must originate from renewable sources. This necessity reinforces the importance of a sustained and coordinated strategy for the large and micro-scale integration of clean energy generation within the EU. Given the inherent intermittency of renewable energy sources, the combination and interaction of multiple generation technologies, supported by energy storage systems, has become essential to achieving a continuous, reliable, and stable energy supply. The development of hybrid renewable energy systems consequently emerges as a key enabler for ensuring energy security and resilience in critical infrastructures, such as ports. Within this context, initiatives such as HY4RES, co-financed by the EU Interreg Atlantic Area Programme, are focused on the implementation and evaluation of micro-scale hybrid renewable systems. One of the selected pilot sites is a Port in Spain, where a hybrid module integrating solar photovoltaic panels, wind turbines, hydrokinetic turbines, and a Pump-as-Turbine (PAT) or battery system is being deployed [4]. The objective is to enhance the energy autonomy and sustainability of port-associated infrastructures through the local generation of renewable electricity. In addition to this project, a total of three additional pilot initiatives are being implemented across Spain, Portugal, and Ireland, addressing sectors that range from agriculture, energy community, and aquaculture to port operations.

Electrifying maritime operations is expected to substantially increase electricity demand across EU ports, making robust energy infrastructure essential to prevent supply shortages. From 2030 onward, studies estimate that port electricity consumption will reach between 6 and 13 TWh per year, highlighting the magnitude of the forthcoming transition [3]. The combined pressures of sustainability targets and rising energy needs indicate that hybrid energy systems will play a central role in future port operations [5]. Their feasibility has already been demonstrated in pilot applications, such as the Port of Souda, where the integration of wind, solar, and storage technologies reduced the LCOE by more than 50% and supplied up to 90% of total energy under optimal conditions [6]. Additional evidence from Egypt shows that hybrid systems are both replicable and cost-effective, with desalination processes benefiting from lower electricity costs and fewer converters compared with single-source renewable configurations [7]. Findings from Ningbo-Zhoushan further reinforce the limitations of isolated renewable technologies, as scenarios relying solely on solar generation exhibited notably poor performance [8]. Space constraints remain a challenge, prompting exploration of offshore hybrid platforms with wind and solar to preserve onshore logistics [9]. Efficient deployment also requires compact, high-energy-density storage, with lithium-ion batteries (75–250 Wh/kg) widely used, though thermal storage often offers superior economic advantages in hybrid setups [10,11]. Growing interest in hydrogen storage, particularly in salt caverns such as Walvis Bay, underscores its potential due to minimal surface footprint and far higher energy density than lithium-ion batteries [12,13]. Efficient operation of hybrid systems reliant on intermittent sources requires advanced management and optimization strategies [14]. Reliable climatic and generation

data, often obtained through predictive systems, are essential, with ensemble learning methods such as stacking regressors (SR) outperforming single models in forecasting solar irradiance and wind speed [15]. Artificial intelligence (AI) plays a central role in hybrid renewable system (HRS) optimization, with 36% of research focusing on AI applications, though metaheuristic approaches still dominate at 47% [16]. AI supports system sizing, consumption prediction, load detection, and shifting, reducing LCOE and emissions—up to 12% in Jeju Island—while mitigating curtailment [17,18]. Complementary tools like digital twins enhance monitoring and energy management, achieving reliability rates of 97% in office buildings, and are applicable to port facilities [19]. Ultimately, in data-scarce environments, optimized initial models are critical, with advanced methodologies refining strategies as more data becomes available.

This broader context has provided the foundation for the development of the present research. The primary objective of this research is to develop a comprehensive energy management and optimization model. The proposed Hybrid Operational Strategy (HOPS) offers several advantages over existing energy management strategies typically applied in port environments: (i) HOPS was developed under a research project and provides a modular and scalable architecture capable of integrating up to five renewable generation sources simultaneously, whereas most existing approaches focus on single-technology or limited hybrid configurations. This flexibility allows the model to adapt to diverse port contexts and evolving technological portfolios; (ii) HOPS incorporates a comprehensive feasibility-assessment framework, processing generation profiles, demand patterns, tariff structures, and component costs within a unified interface. This contrasts with conventional strategies that often require separate tools or lack the ability to evaluate economic, operational, and configuration-based scenarios in an integrated manner; (iii) the model's energy-balance-driven operational logic enables detailed identification of surpluses and deficits, simulation of multiple hybrid configurations, and optimization of operational strategies to ensure economic viability. Existing strategies typically rely on simplified dispatch rules or static assumptions, limiting their capacity to explore dynamic interactions between multiple renewable sources and storage options. Finally, HOPS was designed with accessibility and adaptability in mind, providing a user-friendly interface that supports rapid scenario testing and decision-making. This enhances its practical applicability for port authorities and stakeholders who may not have access to advanced optimization tools. Together, these features position HOPS as a more flexible, comprehensive, and decision-oriented strategy compared with existing hybrid energy management approaches. This model allows for simulation and evaluation of multiple operational scenarios to identify the most efficient configurations and technological combinations, thereby maximizing both the energy performance and economic viability of the hybrid system.

Hence, the remainder of this research work is organized as follows: Section 2 presents the methodology adopted for the development of the Hybrid Operational Strategy (HOPS) model, detailing the refinement of generation data, the definition of demand profiles, and the internal logic of the simulation–optimization framework. It also describes the model architecture, key input parameters, and the structure of the energy management interface. The selected technologies in this research correspond to the configuration of the research project HY4RES pilot system, and the broader applicability of HOPS refers to its modular architecture. Section 3 introduces the configuration of the hybrid renewable energy module, including the characteristics of the photovoltaic, wind, and hydrokinetic systems, as well as the two storage technologies—Pump-as-Turbine and battery systems—evaluated in this research. Section 4 reports the results of the four operational scenarios, comparing the performance of single-module and parallel-module configurations and assessing their energy balance, operational behavior, and economic feasibility. It discusses the implica-

tions of the findings, highlighting the advantages and limitations of each configuration and the practical relevance of the HOPS model for port-energy planning, efficiency and sustainability. Finally, Section 5 summarizes the main conclusions and outlines future research directions, particularly regarding the expansion of HOPS toward more advanced optimization capabilities and broader applicability in port infrastructures.

2. Methodology

To ensure the accurate evaluation and testing of the different scenarios, it has been necessary to analyze the generation values [20]. This review has enabled verification of whether the preliminary estimations are consistent with the results obtained through more refined and advanced calculation methods. The refinement process has represented a key component of the study, as the outcomes of different scenarios depend directly on the hourly generation achieved by each renewable source. Moreover, it has provided the foundation for the development of the energy management and optimization tool implemented in the MS Solver add-in. Accordingly, the adopted methodology comprises the validation of hourly generation data, the selection of demand profiles to be satisfied, and the subsequent definition of the optimization tool's internal logic.

2.1. Energy Management Model Definition and Structure

2.1.1. Energy Management Framework

Accurate and well-structured data on energy generation and demand is fundamental to understanding the dynamics between supply and consumption, enabling a more comprehensive analysis of the system's energy balance. To effectively evaluate and manage these parameters, it is essential to develop a robust analytical tool that offers detailed insights into energy usage, its purposes, patterns, and efficiencies. Such a tool would not only support smarter energy management but also enhance economic outcomes and promote environmental sustainability.

To achieve these objectives, an energy management interface has been developed, selected for its broad accessibility and user-friendly features. The interface offers an intuitive, visually streamlined experience, allowing for efficient control of the hybrid energy module. Designed with flexibility in mind, the tool is both scalable and location-independent, making it suitable for a wide range of deployment scenarios. Whether in urban environments like the one studied or in remote rural areas near rivers or other water sources, the tool adapts seamlessly. By enabling effective energy management across diverse settings, it contributes to more sustainable and efficient energy use on a broader scale.

HOPS is designed as a combined simulation and optimization platform. Its core structure relies on a simulation-based energy balance model that processes generation profiles, demand patterns, tariff structures, and storage behavior. The estimation of output power from photovoltaic, wind, and hydrokinetic systems does not rely on statistical data processing or probability distributions. Instead, the model uses pre-processed hourly generation profiles obtained from validated external tools and datasets obtained in lab tests developed within the HY4RES project. Building on these simulations, HOPS incorporates an optimization layer that evaluates multiple hybrid configurations and operational strategies to identify the most economically viable solution for each scenario. HOPS (Hybrid Operational Strategy) is the platform simulation model developed specifically to support the analysis and optimization of a hybrid energy module. It processes a set of key input parameters, such as energy generation profiles, demand patterns, and tariff structures, alongside a detailed inventory of component quantities and their specific costs. These inputs provide the foundational data necessary for conducting comprehensive feasibility

studies, directly influencing both the economic viability and energy performance of the proposed solution.

Built to be adaptable, HOPS currently supports the integration of up to five generation sources. This study focuses on three primary technologies: photovoltaic, wind, and hydrokinetic power. For energy storage, the tool accommodates either pump-as-turbine systems or battery storage, aligning with the operational scenarios being evaluated. This modular design enables tailored system configurations while maintaining clarity and control over the modeling process.

To enhance its capabilities and broaden its application, HOPS can also be used in Python 3.14.0. With this progress will not only support the integration of additional storage technologies and more complex system architectures but will also enable the implementation of advanced analytical features. By strengthening both functionality and scalability, HOPS is positioned to become a versatile decision-support tool for sustainable energy planning across a wide range of contexts. The underlying logic of the tool is based on the establishment of initial energy balances, which enable the identification of energy surpluses and deficits at any time. From this basis and depending on the available energy resources and storage technologies, the model allows for the simulation of multiple scenarios, whether operating a single module or several in parallel. After evaluating the various configurations supported by the interface, the optimal operational strategy for the hybrid energy module is determined to ensure economic feasibility. In cases where viability cannot be achieved directly, the tool calculates an appropriate energy multiplier ratio to support long-term investment recovery. Figure 1 illustrates the interface logic, from the input of initial data to the generation of final results.

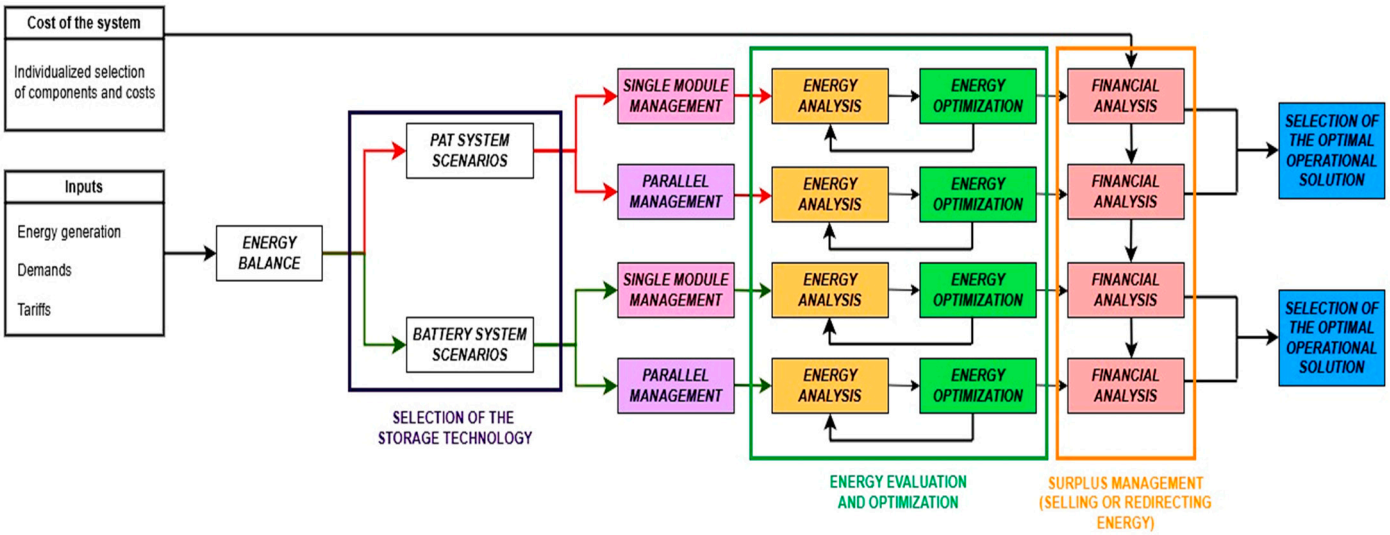

Figure 1. HOPS software logic flow diagram.

2.1.2. Key Parameters

With a clear understanding of the operating logic behind HOPS, it is essential to explore in detail the key components that constitute the tool. This includes a thorough analysis of its inputs, the system's cost breakdown, and the outputs it produces. Given their complexity and centrality, all the scenarios will be addressed individually and comprehensively in future sections.

In any management or computational tool, the quality of the initial inputs is paramount, as they directly influence the accuracy and reliability of the resulting outputs.

In this initial version of HOPS, pre-calculated input data has been deliberately chosen to accelerate scenario simulations and conserve computational resources that would other-

wise be required for real-time generation modeling from various renewable sources. The data has been annualized and structured with hourly granularity to ensure both accuracy and usability in subsequent analyses.

As previously noted, HOPS has been developed to streamline data processing and facilitate swift, accurate decision-making. To support this objective, the number of required inputs for simulations has been strategically limited to three core categories: energy demand, energy generation, and tariff pricing. The interface also incorporates a navigation bar that allows users to easily access different scenarios and sections, an element present across all Excel tabs for intuitive use. Figure 2 provides an overview of the interface, highlighting the section dedicated to data entry for subsequent processing.

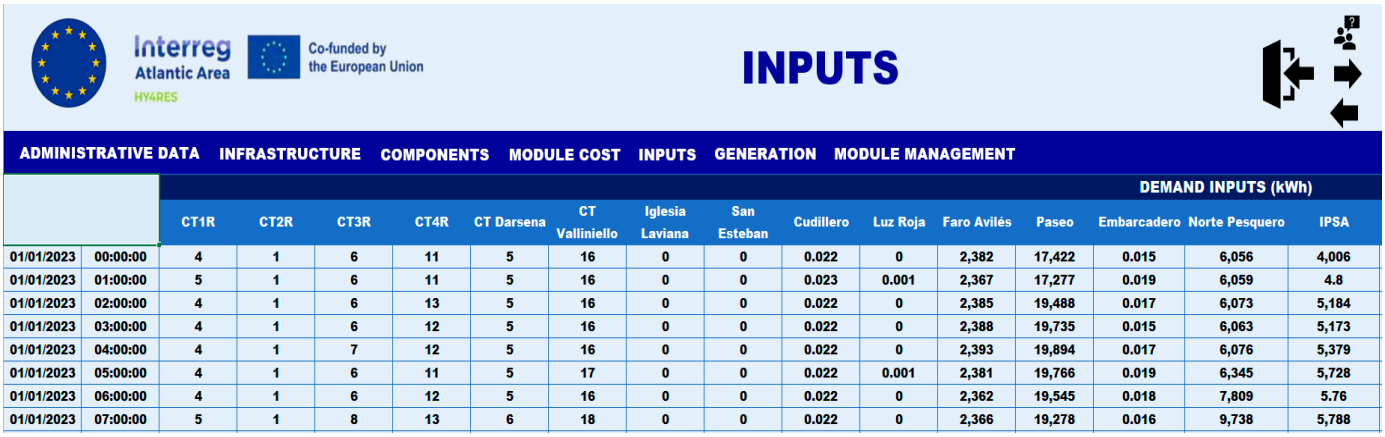

		CT1R	CT2R	CT3R	CT4R	CT Darsena	CT Valliniello	Iglesia Laviana	San Esteban	Cudillero	Luz Roja	Faro Avilés	Paseo	Embarcadero	Norte Pesquero	IPSA
01/01/2023	00:00:00	4	1	6	11	5	16	0	0	0.022	0	2,382	17,422	0.015	6,056	4,006
01/01/2023	01:00:00	5	1	6	11	5	16	0	0	0.023	0.001	2,367	17,277	0.019	6,059	4.8
01/01/2023	02:00:00	4	1	6	13	5	16	0	0	0.022	0	2,385	19,488	0.017	6,073	5,184
01/01/2023	03:00:00	4	1	6	12	5	16	0	0	0.022	0	2,388	19,735	0.015	6,063	5,173
01/01/2023	04:00:00	4	1	7	12	5	16	0	0	0.022	0	2,393	19,894	0.017	6,076	5,379
01/01/2023	05:00:00	4	1	6	11	5	17	0	0	0.022	0.001	2,381	19,766	0.019	6,345	5,728
01/01/2023	06:00:00	4	1	6	12	5	16	0	0	0.022	0	2,362	19,545	0.018	7,809	5.76
01/01/2023	07:00:00	5	1	8	13	6	18	0	0	0.022	0	2,366	19,278	0.016	9,738	5,788

Figure 2. Input data entry screen in HOPS.

HOPS currently supports the entry of up to twenty-three demand points, from which users must identify those that could be served by one or more hybrid modules. From the total of twenty-three consumption points, up to three profiles can be analyzed simultaneously. These profiles can either be grouped together and assigned to a single hybrid module or allocated across three separate modules in parallel configurations. To streamline the process and minimize the need to navigate back to the inputs tab, drop-down menus are available, allowing for efficient selection of the desired profiles, as demonstrated in Figure 3.

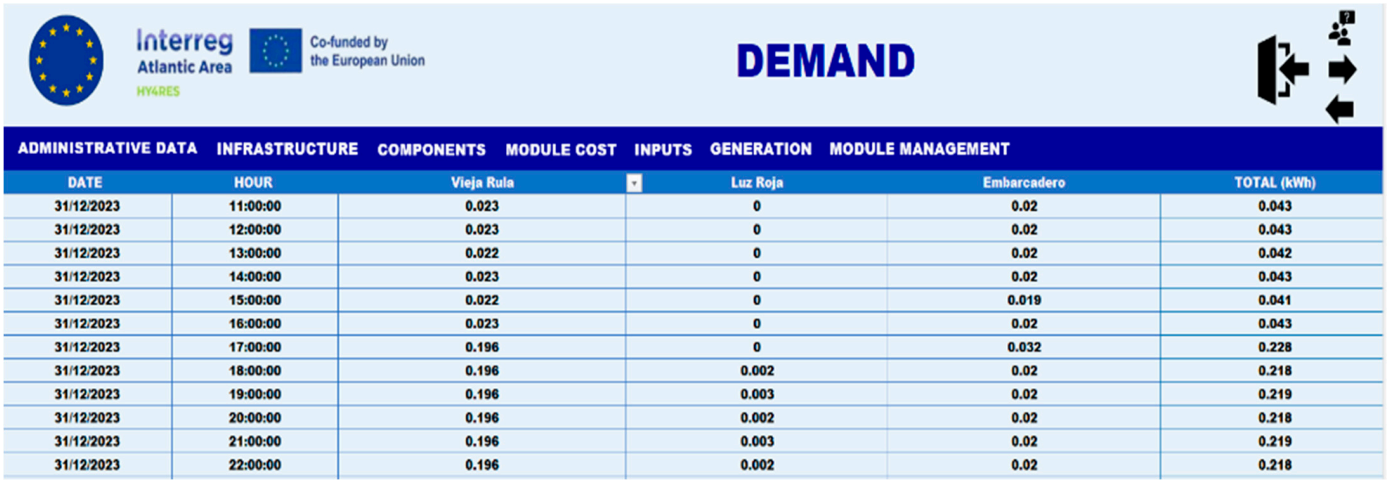

DATE	HOUR	Vieja Rula	Luz Roja	Embarcadero	TOTAL (kWh)
31/12/2023	11:00:00	0.023	0	0.02	0.043
31/12/2023	12:00:00	0.023	0	0.02	0.043
31/12/2023	13:00:00	0.022	0	0.02	0.042
31/12/2023	14:00:00	0.023	0	0.02	0.043
31/12/2023	15:00:00	0.022	0	0.019	0.041
31/12/2023	16:00:00	0.023	0	0.02	0.043
31/12/2023	17:00:00	0.196	0	0.032	0.228
31/12/2023	18:00:00	0.196	0.002	0.02	0.218
31/12/2023	19:00:00	0.196	0.003	0.02	0.219
31/12/2023	20:00:00	0.196	0.002	0.02	0.218
31/12/2023	21:00:00	0.196	0.003	0.02	0.219
31/12/2023	22:00:00	0.196	0.002	0.02	0.218

Figure 3. HOPS interface for demand profile selection.

Furthermore, a dedicated tab is included to graphically display the profiles, allowing users to assess their behavior, identify usage patterns, and, at an early stage, pinpoint periods during the year when the hybrid module may experience higher demand or when a greater portion of the system's storage capacity might be needed. In addition to the visual representation, the tool provides monthly and annual values for each profile, as well as the percentage contribution of each demand relative to the total consumption of the three selected profiles. The discretization of the demand profiles is directly determined by the availability and granularity of the real port data.

As with the selected consumption points, the generation units offer a graphical representation of their profiles and the corresponding impact on the total system (Figure 4). The key difference is that, since a maximum of five energy production systems can be entered, there is no need for users to individually select each technology. Instead, all available generation sources are displayed within the interface. If fewer than five sources are utilized, any unfilled columns are automatically interpreted as representing zero production, maintaining the system's flexibility.

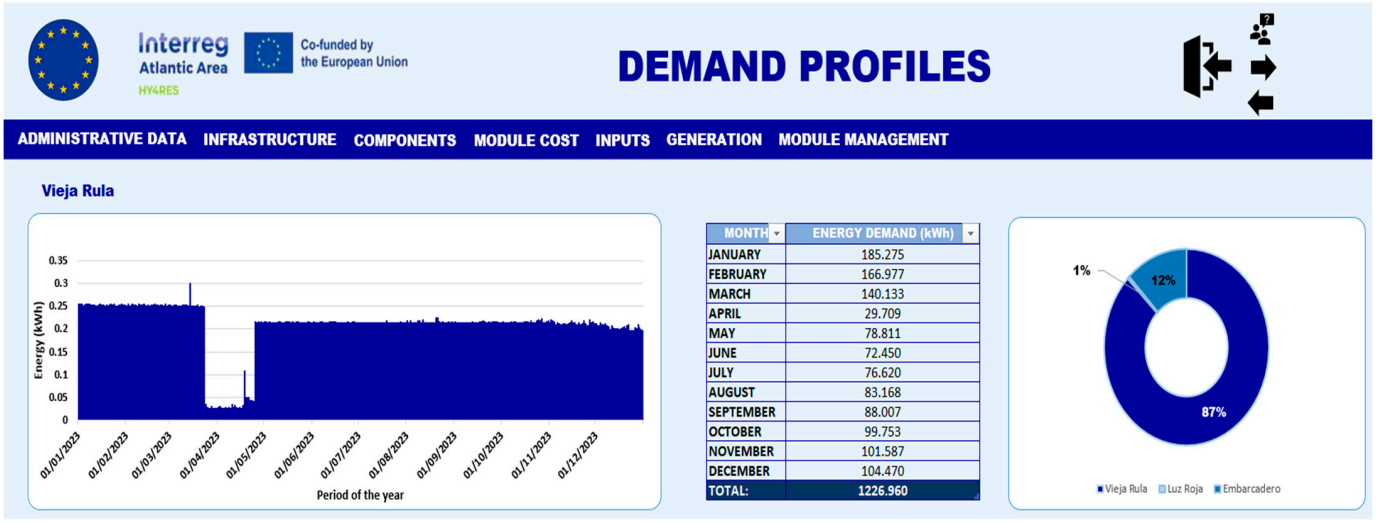

Figure 4. HOPS interface for demand profile visualization.

Regarding the selection of the tariff model, it is currently aligned with the structure established in Spain, requiring the input of period-specific electricity prices based on utility bills for each infrastructure. In scenarios where multiple consumption points are associated with different electricity providers, resulting in varying rates, either an average tariff must be calculated, or separate simulations should be conducted for each infrastructure. These values are critical, as they significantly influence the economic outputs of the analysis; therefore, their accurate definition is essential to properly assess the overall viability of the system's implementation.

2.2. Validation of Actual Generation Data

The validation process of the energy production data from the different sources comprising the hybrid module begins with the definition of the characteristics and performance ratios used, together with the results obtained from the preliminary design phase in which the project was conceived. All these data are presented in Table 1, which serves as a reference for subsequent comparison with the results derived from alternative calculation methods.

Table 1. Preliminary characteristics and outcomes defined in the base case.

	Photovoltaic Unit	Wind Unit	Hydrokinetic Unit	PAT Unit
Power per installed component (W)	405	800	-	200
Number of components	2	3	2	1
Total power installed (W)	810	2400	-	200
Average solar irradiation (kWh/m^2/day)	3	-	-	-
Area swept by turbine (m^2)	-	0.45	0.28	-
Average wind potential (W/m^2)	-	250	-	-
Average water velocity (m/s)	-	-	0.7	-
Energy Generated (kWh/year)	567.65	473.04	135.55	140.16
Contribution (%)	43%	36%	10%	11%

It is worth mentioning that the literature utilization factors (30–33% for PV and 40–60% for wind) correspond to large-scale, utility-level installations operating in optimal conditions. In contrast, the systems analyzed in this research are micro-generation units installed in a port environment, where (i) wind conditions are highly variable and often turbulent due to surrounding infrastructure, (ii) the small wind turbine has a higher cut-in speed and lower aerodynamic efficiency, and (iii) the PV panels operate closer to their nominal performance under the local climate. Based on the data presented in Table 1, it was observed that the use of annual averaged values extrapolated over an entire year could lead to potential discrepancies when estimating total energy production, since wind speed, solar irradiation, and tidal activity are not uniform over time. To address this limitation, the adopted approach focused on obtaining hourly data for both solar irradiation and wind speed, as well as identifying tidal patterns that would allow the determination of the operational windows for the hydrokinetic turbines. This information was sourced from PVGIS [21] (for irradiation and wind data) and the PORTUS database (for tidal cycle analysis) [22].

By following the generation ratios defined with a customized hourly approach, a much more realistic treatment of the data is enabled. Different methodologies were then applied to estimate the energy generation from each renewable source. For the photovoltaic system, PVsyst 8 software, widely used in the industry, was employed, as it allows for detailed modeling including near-shading profiles, electrical and thermal losses, and professional layout design with optimized panel tilt and orientation.

For the wind energy unit, given that residential-scale wind turbines were used, it was more challenging to identify software capable of accurately modeling energy generation. Therefore, the turbine's power curve was estimated as a function of wind speed, using its commercial specifications: cut-in speed (2 m/s), nominal power speed (11 m/s), and cut-out speed (25 m/s). A trend line was then derived, resulting in Equation (1), from which the hourly power extracted from the turbine (P_{turb}) was calculated using the wind speed data (v) obtained from PVGIS.

$$P_{turb} = 0.0002 \cdot v^6 - 0.0153 \cdot v^5 + 0.5673 \cdot v^4 - 10.112 \cdot v^3 + 82.934 \cdot v^2 - 185.33 \cdot v + 111.66 \quad (1)$$

For the hydrokinetic unit, its operational behavior has been defined based on the periodic variation of tidal flow velocities, which occur in six-hour cycles, between higher and lower speeds. Using this information, together with the generation values per square meter identified in previous studies for the Port of Avilés, it was determined that the turbines operate for six consecutive hours followed by six hours of inactivity, resulting in a generation rate of 0.0995 kWh/m^2, for the specific location where the module has been implemented [23,24].

Considering all the criteria and processes discussed, the application of more advanced methodologies and analytical procedures resulted in an energy generation output 253% higher than the initial estimates based on fixed ratios. This outcome clearly demonstrates that the variability of renewable energy sources cannot be accurately represented by a static value. The detailed results are presented in Table 2.

Table 2. Final source contribution with the application of alternative calculation methodologies.

	Photovoltaic Unit	Wind Unit	Hydrokinetic Unit
Total power installed (W)	810	2400	75
Energy generation (kWh)	784.73	2309.03	244.05
Coverage (%)	24%	69%	7%

2.3. Demand Profile Selection

The selection of demand profiles constitutes another key factor that defines the methodology and directly influences the optimization of the hybrid module, together with the associated tariff structures. Among the 23 consumption points for which energy demand data were available for the year 2023, those that best matched the generation scale of the hybrid module were selected. Of these, only three were found to fall within the coverage capabilities of the designed renewable generation system, all of which were assigned to the 2.0TD tariff category, typically applied to low-demand infrastructures. The remaining facilities exhibited significantly higher demand levels, making the use of energy storage at those points unnecessary, as all available generation would be fully utilized to meet as much demand as possible. Under such conditions, it would be difficult to effectively evaluate the operational functionality of the hybrid system.

The total annual energy to be supplied, derived from the sum of the selected demand profiles, amounts to approximately 1405.17 kWh, which falls well within the generation range of the module. Although the associated tariffs do not directly influence the system's energy performance, they have a notable impact on the economic recovery of the investment. In addition to selling surplus energy to the grid, the feasibility of redistributing excess generation to infrastructures operating under higher-cost tariff categories, specifically the 3.0TD tariff, has been studied. Figure 5 shows the energy profiles for the selected infrastructures.

2.4. Definition of the Energy Management and Optimization Tool

Energy generation, demand, and tariff values constitute essential inputs for the operation of the developed optimization tool. Its core logic is based on identifying energy surpluses and deficits from an initial energy balance, which are subsequently managed according to the available storage capacities of either the PAT or battery systems at each hour.

Using this balance and the selected storage technology, the tool evaluates multiple configurations, both individual and parallel, to assess energy performance and determine the optimal number of renewable components to install, through a parameter called units multiplier, together with the storage capacity. The objective is to satisfy predefined coverage targets while maximizing economic efficiency through financial analysis.

The optimization process is subject to spatial constraints (available surface area for module installation), maximum investment limits, and minimum coverage requirements from direct renewable generation and storage contribution. Considering these restrictions and the defined module costs, the tool calculates the cost per installed kW for each source and allocates resources to achieve optimal compliance. Finally, by applying predefined surplus management strategies, such as redirecting excess energy to higher-tariff infrastructures or selling it to the grid, the model identifies the configuration that yields the highest economic return while meeting all technical performance criteria. The following

Figure 6 presents the optimization schemes for both single-module (M1) and multi-module (M1-M2-M3 in parallel) configurations.

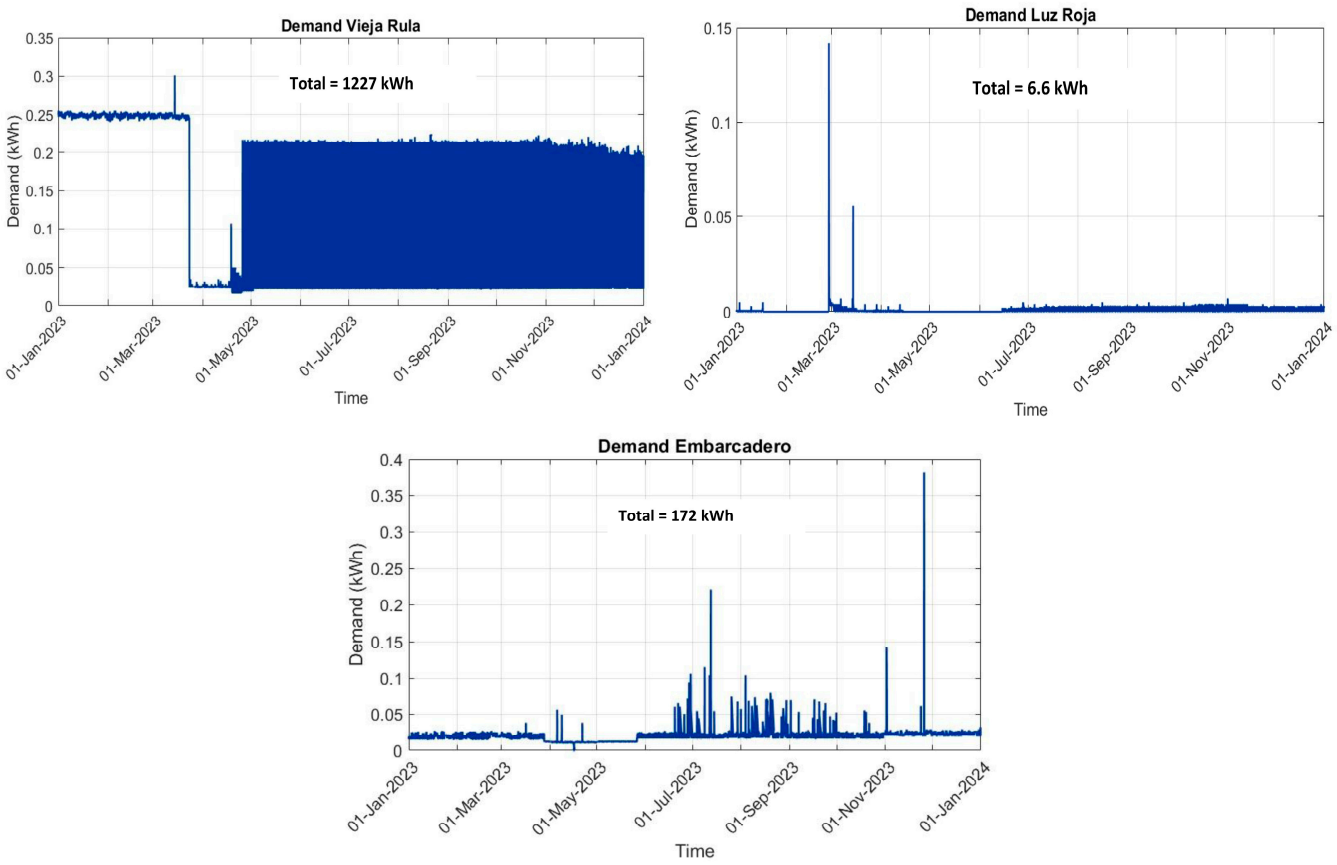

Figure 5. Selected demand profiles and total consumptions in kWh.

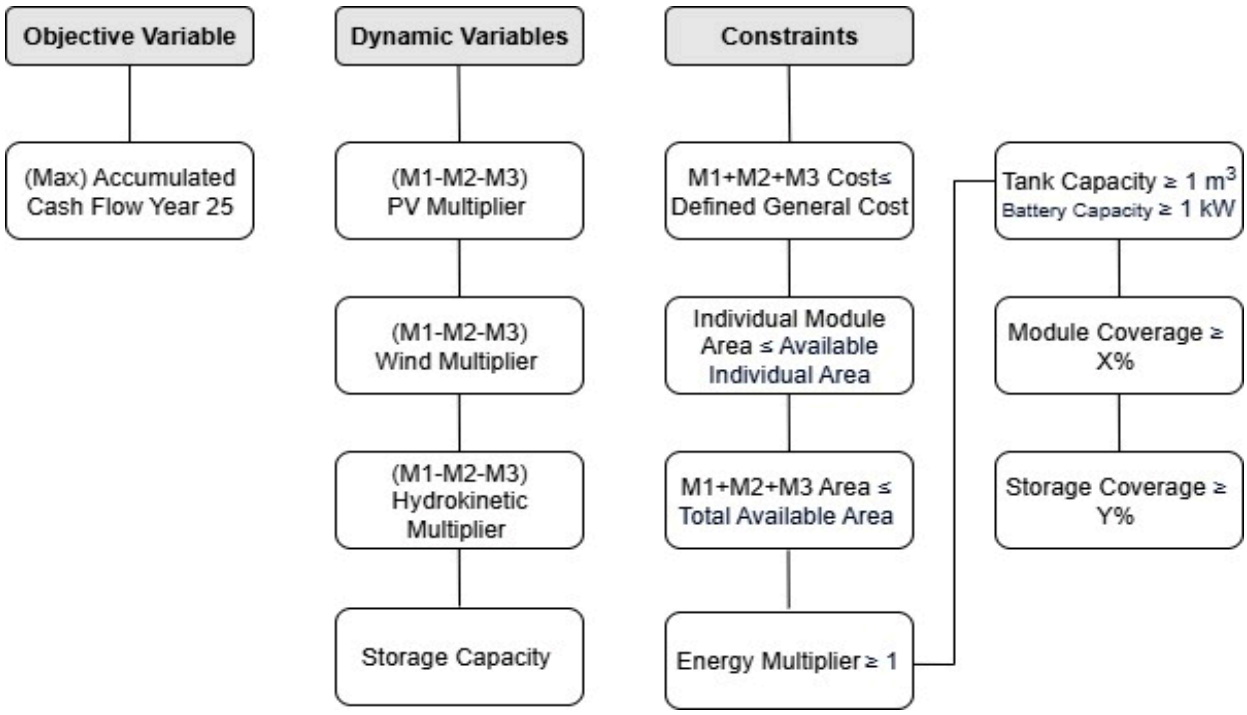

Figure 6. Optimization scheme for individual (M1) and parallel (M1-M2-M3) configurations.

3. Scenario Definition and Formulations

Following the definition of the methodology used to obtain the input data and the description of the operation of the energy management and optimization tool, the characteristics of each tested scenario are presented. Four scenarios are defined to reflect the real decision-making needs of the HY4RES pilot installation and to evaluate the performance of the HOPS model under progressively more complex operational configurations: (i) The first two scenarios assess the behavior of a single hybrid module using each storage technology independently (battery and PAT). These scenarios establish the baseline performance of each storage option and allow a direct comparison of their technical and economic feasibility. (ii) The next two scenarios evaluate parallel configurations, where multiple modules operate simultaneously. These scenarios are essential because the pilot system may need to supply more than one demand energy sector point, and parallel operation introduces additional challenges related to energy sharing, storage coordination, and system scalability. One scenario considers independent storage units for each module, while the other evaluates a shared, centralized storage system.

Together, these four scenarios represent the full range of realistic operational configurations for the pilot system and allow the HOPS model to be tested under both simple and complex conditions.

3.1. Scenario 1: Single Module with PAT System

Scenario 1 is based on the use of a single module to supply energy to the three selected consumption profiles. The particularity of this scenario lies in the use of the PAT as an energy storage solution. This configuration requires consideration of several additional factors during testing, such as the efficiency of the PAT system (η_{PAT}), assumed here to be 60%, and the elevation of the tank (H), which is positioned approximately 5 m above ground level. When employing a storage system of this nature, the process necessarily involves a conversion between volume (V) and energy. Consequently, the energy balance expressed in Equation (2) must be complemented by Equation (3) [24,25], ensuring the correct conversion between the energy balance ($E_{NET,t}$) and the corresponding volume to be stored.

$$E_{NET,t} = (E_{PV,t} + E_{WIND,t} + E_{HYDRO,t}) - E_{LOAD,t} \quad (2)$$

$$V = \frac{E_{Sur,t} \cdot 3.6 \cdot 10^6}{\eta_{PAT} \cdot \rho \cdot g \cdot H} \quad (3)$$

For this scenario, four operational stages have been defined for the module: a tank charging phase, a discharging phase, a deficit identification phase, which detects any remaining unmet demand that must be supplied by the grid, and, finally, the determination of the tank's current state. Additional relevant parameters in this operational framework include the initial tank volume, set at 50% of its estimated capacity during the first operational hour, and the maximum discharge limit, established to prevent cavitation and other undesired events. In this case, the system is designed to always maintain a minimum of 5% of the tank's total capacity.

Determining when the storage tank can be charged begins with referencing the initial energy balance defined in Equation (4). This balance serves as the key indicator of whether surplus energy is available for storage or if a deficit must be covered using the tank's reserves. Within the simulation and optimization framework, system operation adheres to a core principle: surplus energy shall not be exported unless the storage tank has reached its maximum capacity. This approach reflects the system's overarching objective of maximizing energy self-sufficiency and minimizing reliance on external sources.

To enable the management model to determine tank charging and surplus energy allocation, a set of governing equations has been defined. These ensure proper operation of the hybrid module according to the available energy at each time step. The formulation differs between the initial hour, which relies on predefined conditions, and subsequent hours, which depend on the preceding system state. Since charging must be interpreted in both energy and volume terms, the conversion in Equation (3) is applied.

$$V_{fill,0} = \begin{cases} \left| \frac{E_{NET,0} \cdot 3{,}600{,}000}{\rho \cdot g \cdot H} \right|, \text{if } E_{NET,0} > 0 \text{ and } \left| \frac{E_{NET,0} \cdot 3{,}600{,}000}{\rho \cdot g \cdot H} + V_{max} \cdot \frac{V_{50\%}}{100} \right| < V_{max} \\ 0, \text{otherwise} \end{cases} \quad (4)$$

where $V_{fill,0}$ denotes the water volume allocated to the tank in the initial time step (m^3), V_{max} is the maximum tank capacity (m^3), $V_{50\%}$ refers to the 50% of tank capacity (m^3), and $E_{NET,0}$ corresponds to the net energy balance at the initial time step (kWh). Equation (4) specifies that when the initial energy balance is positive and the combined volume of the storable surplus and the initial tank level remains within the tank's maximum capacity, the full surplus volume is stored. If either condition is not met, no energy is allocated to the tank, and storage remains unchanged.

For all subsequent time steps, the same logic applies but is adapted to the system's evolving state. Tank charging depends on the residual volume from the previous hour, and the surplus energy generated in the current hour. However, full utilization is possible only when the surplus does not exceed the remaining capacity; otherwise, only the storable portion is used, with any excess managed according to the predefined strategy. This charging logic for successive hours is formalized in Equation (5).

$$V_{fill,t} = \begin{cases} \left| \frac{E_{NET,t} \cdot 3{,}600{,}000}{\rho \cdot g \cdot H} \right|, \text{if } E_{NET,t} > 0 \text{ and } \left| \frac{E_{NET,t} \cdot 3{,}600{,}000}{\rho \cdot g \cdot H} \right| + V_{rem,t-1} < V_{max} \\ V_{max} - V_{rem,t-1}, \text{if } E_{NET,t} > 0 \text{ and } \left| \frac{E_{NET,t} \cdot 3{,}600{,}000}{\rho \cdot g \cdot H} \right| + V_{rem,t-1} > V_{max} \\ 0, \text{if } E_{NET,t} \leq 0 \end{cases} \quad (5)$$

In this equation, $V_{fill,t}$ corresponds to the volume of water assigned to fill the tank at a specific time step (m^3), $E_{NET,t}$ refers to the net energy balance at that specific time step (kWh) and $V_{rem,t-1}$ indicates the remaining volume in the tank from the previous time step (m^3). All other variables retain the definitions provided in the preceding equations.

While tank loading serves as a cornerstone in defining the energy model, robust deficit management is equally essential to ensure reliable operation of the hybrid system. In periods of insufficient renewable generation, the PAT system must be leveraged to deliver the maximum feasible energy output, all while preserving the technical integrity and economic viability of the overall configuration.

Before assessing the extent to which the storage system can compensate for the energy deficit, it is crucial to first evaluate the actual volume demand, factoring in the inherent inefficiencies of the system. As previously discussed, various loss factors within the PAT system can significantly impact performance. These must be thoroughly accounted for to ensure the accuracy of all estimations and to prevent operational misjudgements that could compromise the reliability of the results.

To accurately reflect system inefficiencies, the efficiency parameter is incorporated into the calculation of the water volume required to cover the energy deficit for a given hour. For instance, if the system operates at 60% efficiency, a proportionally higher volume of water must be discharged from the tank to deliver the required energy output. This efficiency factor, along with other critical parameters such as hydraulic head, is fully configurable by the user, ensuring adaptability to a wide range of system specifications. The quantitative

relationship between water volume required, $V_{need,t}$ (m^3), and net energy is formalized through Equation (6).

$$V_{need,t} = \begin{cases} \left| \frac{E_{NET,t} \cdot 3{,}600{,}000}{\eta_{PAT} \cdot \rho \cdot g \cdot H} \right|, E_{NET,t} < 0 \\ 0, \text{otherwise} \end{cases} \quad (6)$$

Once the water volume necessary to cover the rest of the demand is defined, the discharge volume, $V_{disch,0}$ (m^3), for the initial time step and, $V_{disch,t}$ (m^3), for subsequent ones, must be determined to generate energy through the turbine. This discharge depends on the storage level at each step and must respect the user-defined minimum threshold, $V_{5\%}$ (m^3). The conversion from energy deficit to water volume remains constant, as it is independent of the tank's state. Moreover, discharge behavior differs between the first hour and later steps: the initial condition follows user-defined parameters, Equation (7), while subsequent discharges depend on the storage level from the preceding hour, Equation (8).

$$V_{disch,0} = \begin{cases} V_{need,0} & , \text{ if } V_{max} \cdot \left(\frac{V_{50\%}}{100} \right) \geq V_{need,0} \text{ and } V_{max} \cdot \left(\frac{V_{50\%}}{100} \right) - V_{need,0} > V_{max} \cdot \left(\frac{V_{5\%}}{100} \right) \\ V_{max} \cdot \left(\frac{V_{50\%}}{100} \right) - V_{max} \cdot \left(\frac{V_{5\%}}{100} \right), & \text{otherwise} \end{cases} \quad (7)$$

$$V_{disch,t} = \begin{cases} 0 & , \text{ if } V_{rem,t-1} = V_{max} \cdot \left(\frac{V_{5\%}}{100} \right) \text{ or } E_{NET,t} \leq 0 \\ V_{need,t} & , \text{if } V_{rem,t-1} - V_{max} \cdot \left(\frac{V_{5\%}}{100} \right) \geq V_{need,t} \\ V_{rem,t-1} - V_{max} \cdot \left(\frac{V_{5\%}}{100} \right) & , \text{ if } \left(V_{need,t} > V_{rem,t-1} \text{ or } V_{rem,t-1} - V_{max} \cdot \left(\frac{V_{5\%}}{100} \right) < V_{need,t} \right) \\ \text{and } V_{rem,t-1} \geq V_{max} \cdot \left(\frac{V_{5\%}}{100} \right) & \end{cases} \quad (8)$$

Once the tank's charging and discharging dynamics have been defined, the next step is to assess the system's energy balance following the operation of the PAT system. This evaluation determines whether the energy supplied by the storage system is sufficient to meet the previously identified deficit, or if a residual shortfall must be covered by the electricity grid. The analysis involves comparing the estimated energy demand with the energy equivalent of the volume discharged from the tank. This is achieved through a volume-to-energy conversion, ensuring that the discharged volume corresponds accurately to the initial deficit. The process is formally controlled by Equation (9), defining the energy in terms of volume, $V_{cov,t}$ (m^3), that cannot be covered through the storage system.

$$V_{cov,t} = \begin{cases} V_{need,t} - V_{disch,t}, & \text{if } V_{need,t} > V_{disch,t} \\ 0, & \text{if } V_{need,t} \leq V_{disch,t} \end{cases} \quad (9)$$

Ultimately, defining the final state of the tank after the charging and discharging processes is critical, as each time step is intrinsically linked to the previous one, and the available storage at the end of a given hour—$V_{rem,0}$ (m^3) for the initial time step and $V_{rem,t}$ (m^3) for the following ones—determines the operational flexibility for the next. Although the model's logic has been presented in a structured sequence, with the final volume determination appearing as the last phase, it is important to recognize that the system functions through continuous, bidirectional interactions. Therefore, the sequence serves more as a conceptual framework than a rigid procedural order. Among all components of the model, the control of the final tank state is the most complex, requiring the greatest number of equations, as it must dynamically account for both energy surpluses and deficits across all time steps, as can be seen in Equations (10) and (11).

$$V_{rem,0} = \begin{cases} V_{max} \cdot \left(\frac{V_{50\%}}{100}\right) + V_{fill,0} & , \text{ if } V_{fill,0} > 0 \\ V_{max} \cdot \left(\frac{V_{50\%}}{100}\right) - V_{need,0} & , \text{ if } V_{max} \cdot \left(\frac{V_{50\%}}{100}\right) - V_{need,0} \geq V_{max} \cdot \left(\frac{V_{5\%}}{100}\right) \\ V_{max} \cdot \left(\frac{V_{5\%}}{100}\right) & , \text{ if } V_{max} \cdot \left(\frac{V_{50\%}}{100}\right) - V_{need,0} < V_{max} \cdot \left(\frac{V_{5\%}}{100}\right) \\ V_{max} \cdot \left(\frac{V_{50\%}}{100}\right) + V_{fill,0} - V_{need,0} & , \text{ if } V_{max} \cdot \left(\frac{V_{50\%}}{100}\right) + V_{fill,0} - V_{need,0} < V_{max} \\ V_{max} & , \text{ if } V_{max} \cdot \left(\frac{V_{50\%}}{100}\right) + V_{fill,0} - V_{need,0} \geq V_{max} \end{cases} \quad (10)$$

$$V_{rem,t} = \begin{cases} V_{max} \cdot \left(\frac{V_{5\%}}{100}\right) & , \text{ if } V_{rem,t-1} + V_{fill,t} - V_{need,t} \leq V_{max} \cdot \left(\frac{V_{5\%}}{100}\right) \\ V_{rem,t-1} + V_{fill,t} - V_{need,t} & , \text{ if } V_{rem,t-1} + V_{fill,t} - V_{need,t} < V_{max} \\ V_{max} & , \text{ if } V_{rem,t-1} + V_{fill,t} - V_{need,t} \geq V_{max} \\ \text{with} V_{rem,t+1} \geq 5\% \, V_{max} & , \forall t \end{cases} \quad (11)$$

The optimization and distribution of resources are constrained by financial, spatial, and energy coverage limitations. In this case, the maximum available budget is set at 25,000 €, the usable area is limited to 100 m^2, and it is established that at least 70% of the total demand must be met through renewable generation and the use of the PAT system.

Efficient surplus energy management is critical to optimizing the financial performance of energy projects and shortening the return on investment period. A particularly promising strategy involves selling excess energy, those amounts not captured by the storage system, to the grid [26,27]. This enables the creation of an additional revenue stream and enhances overall project profitability. Surplus energy fed into the grid is typically compensated at rates lower than the retail purchase price. Therefore, selecting an energy off-taker that offers the most favorable compensation rate is essential to maximizing the economic viability of this strategy. In the context of the current case study, the assumed sale price is based on the simplified compensation mechanism applicable to grid-connected self-consumption photovoltaic systems in Spain. This mechanism generally offers compensation in the range of 0.05 €/kWh to 0.10 €/kWh. For modeling purposes, a representative midpoint value of 0.07 €/kWh has been adopted. To clarify the relationships and energy flows between the various agents involved in this scheme, a flow diagram has been developed and is presented in Figure 7.

To evaluate the effectiveness of the proposed strategy, a comprehensive economic model has been developed. This model quantifies, first, the annual cost savings achieved through reduced electricity purchases, based on the tariff structure detailed in the Methodology Section. Second, it estimates the additional revenue generated from the sale of surplus energy to the grid, providing a complete picture of the strategy's financial impact.

The annual cost savings and revenue from surplus energy sales serve as the primary indicators of the strategy's economic performance, directly influencing the investment's payback period. In this study, financial projections are extended over a 25-year horizon, aligned with the estimated operational lifespan of the hybrid module.

By analyzing the energy purchase prices across different periods and tariff models, as detailed in the Methodology Section, in conjunction with the average energy sale price, it has been determined that an alternative approach could potentially optimize the benefits from surplus energy management.

Considering the relatively low energy sale price and the structure of tariffs such as 3.0TD, where, during certain periods, energy purchase costs can exceed the sale price by up to threefold, an effective strategy would be to redirect surplus energy to high-demand areas within the port. This would significantly enhance economic savings by maximizing self-consumption where the cost differential is greatest. Additionally, this approach would reduce reliance on the external grid, leading to fewer transactions between the hybrid module and the network. As a result, it would

not only lower emissions but also decrease grid demand for both the targeted infrastructures and other buildings subject to the 3.0TD tariff, amplifying the overall environmental and economic benefits. Taking into account the specific modification of reallocating surplus energy, the remaining calculations from the previous strategy will remain unchanged. The same evaluation criteria and performance indicators will be applied to assess the viability of this revised approach, once all technical and economic parameters of the case study have been defined. Figure 8 illustrates the updated flow graphic, outlining the operational adjustment incorporated into the strategy.

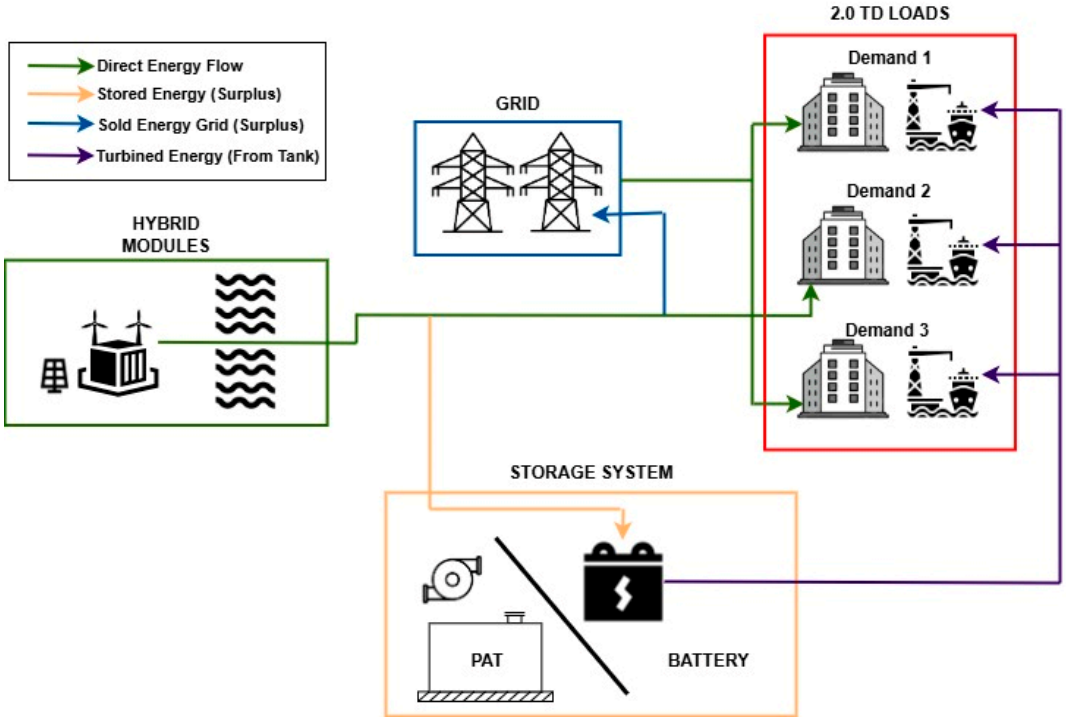

Figure 7. Directional energy flow for strategic selling of surplus energy using.

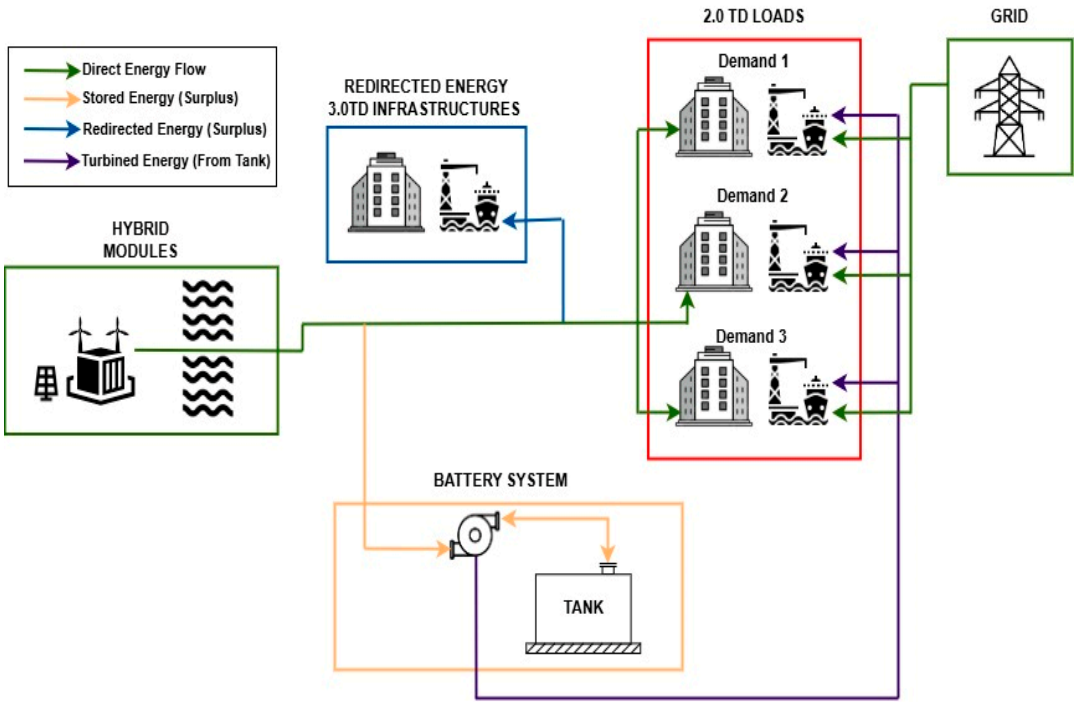

Figure 8. Directional energy flow for strategic redistribution under 3.0TD tariff, using PAT system.

It is important to note that these two surplus management strategies will be applied consistently across all scenarios [28,29]. Therefore, from this point onward, only the economic outcomes resulting from the implementation of both strategies will be presented, with an emphasis on identifying the most advantageous option in each case.

3.2. Scenario 2: Single Module with Battery System

Scenario 2 aims to evaluate whether the use of batteries as an energy storage system proves to be more advantageous compared to the PAT-based configuration, while maintaining the installation of a single module to cover the three selected consumption profiles. One of the main distinctions in this case is that the process does not involve any conversion between volume and energy, which considerably simplifies the testing of this scenario. Similar to Scenario 1, an initial state of charge of 50% of the total storage capacity is defined, along with a maximum Depth of Discharge (DoD) set at 97%.

One of the main advantages of using batteries compared to the PAT system is that their operation requires fewer components. In this case, there is no need for a storage tank, a reversible pump-turbine, or the associated piping and valve system that constitutes the PAT setup. This reduction in system complexity not only lowers the overall investment requirements but also significantly decreases the physical space needed.

To ensure consistency and enable a realistic comparison between Scenarios 1 and 2, the same investment level of 25,000 €, the same available area of 100 m^2, and a minimum coverage requirement of 70% are maintained.

The battery charging process follows the same fundamental logic applied to the tank in Scenario 1, with modifications tailored to the specific technical characteristics of battery storage systems. Charging is initiated when renewable energy generation exceeds the system's demand during a given time step, resulting in a surplus. Once this surplus is detected, the system determines whether it can be stored, subject to defined lower and upper operational limits. A maximum threshold, established by the battery's technical specifications, ensures that the system does not exceed its permissible storage capacity.

This control logic is formalized in Equations (12) and (13), which adopt a structure similar to that used in Scenario 1. As with the PAT-based model, a clear distinction between the first time step, $B_{charge,0}$ (kWh), and subsequent intervals, $B_{charge,t}$ (kWh), is maintained throughout the simulation, ensuring continuity in the system's dynamic behavior.

$$B_{charge,0} = \begin{cases} E_{NET,0} & , \text{ if } E_{NET,0} > 0 \text{ and } E_{NET,0} + \left(B_{max} \cdot \frac{SoC_{50\%}}{100}\right) < B_{max} \\ B_{max} \cdot \left(1 - \frac{SoC_{50\%}}{100}\right) & , \text{ if } E_{NET,0} > 0 \text{ and } E_{NET,0} + \left(B_{max} \cdot \frac{SoC_{50\%}}{100}\right) \geq B_{max} \\ 0 & , \text{ if } E_{NET,0} < 0 \end{cases} \quad (12)$$

$$B_{charge,t} = \begin{cases} E_{NET,t}, & \text{if } E_{NET,t} > 0 \text{ and } SoC_{,t} + E_{NET,t} \leq B_{max} \\ B_{max} - SoC_{,t}, & \text{if } E_{NET,t} > 0 \text{ and } SoC_{,t} + E_{NET,t} > B_{max} \\ 0, & \text{if } E_{NET,t} \leq 0 \end{cases} \quad (13)$$

In these equations, B_{max} (kW) refers to the battery maximum capacity, and $SoC_{50\%}$ corresponds to the state of charge of the battery at 50% of the total capacity.

3.2.1. Battery Discharge

Regarding battery discharge, this process is governed by Equations (14) and (15). Just as with battery charging, it is essential to define clear operational limits. In this case, the maximum allowable discharge, previously set by the user, must be strictly controlled to ensure compliance with established safety requirements.

$$B_{disch,0} = \begin{cases} |E_{NET,0}|, \text{ if } E_{NET,0} \leq 0 \text{ and } B_{max} \cdot \left(\frac{Soc_{50\%}}{100}\right) - |E_{NET,0}| \geq B_{max} \cdot \left(\frac{100 - DoD_{97\%}}{100}\right) \text{ and } E_{NET,0} \leq P_{max} \\ 0, \text{ if } E_{NET,0} < 0 \text{ and } B_{max} \cdot \left(\frac{Soc_{50\%}}{100}\right) - |E_{NET,0}| < B_{max} \cdot \left(\frac{100 - DoD_{97\%}}{100}\right) \\ 0, \text{ if } E_{NET,0} > 0 \end{cases} \quad (14)$$

$$B_{disch,t} = \begin{cases} |E_{NET,t}|, \text{ if } E_{NET,t} < 0 \text{ and } SoC_{t-1} - |E_{NET,t}| \geq B_{max} \cdot \left(\frac{100 - DoD_{97\%}}{100}\right) \text{ and } E_{NET,t} \leq P_{max} \\ SoC_{t-1} - B_{max} \cdot \left(\frac{100 - DoD_{97\%}}{100}\right), \text{ if } E_{NET,t} < 0 \text{ and } SoC_{t-1} - |E_{NET,t}| < B_{max} \cdot \left(\frac{100 - DoD_{97\%}}{100}\right) \\ 0, \text{ if } E_{NET,t} \geq 0 \end{cases} \quad (15)$$

The formulation of Equations (14) and (15) is marked by the definition of the battery discharge at the initial state, $B_{disch,0}$ (kWh), the maximum power of the battery that can be discharged in one hour, P_{max} (kW), the maximum depth of discharge allowable, $DoD_{97\%}$, the discharge of the battery in the subsequent time steps, $B_{disch,t}$ (kWh), and the state of charge from the previous time step, SoC_{t-1} (kW). The rest of the variables have been defined before.

3.2.2. State of Charge Management

Accurately determining the battery state of charge is fundamental to the proper functioning of the system, as it directly influences subsequent charging and discharging operations. Any error in estimating the SoC can compromise the performance of the hybrid module, particularly if surplus energy is not managed as intended, resulting in system behavior that deviates from expected outcomes. The definition of the battery state of charge is considerably more straightforward compared to the PAT configuration involving a tank-based storage system. This highlights one of the key simplifications achieved in the development of the management model, enabled solely by modifying the type of storage employed. This change not only reduces system complexity but also facilitates more seamless interactions between the various operational processes, as detailed in Equations (16) and (17).

$$SoC_{,0} = \left(B_{max} \cdot \frac{SoC_{50\%}}{100}\right) + B_{charge,0} - B_{disch,0} \quad (16)$$

$$SoC_{,t} = SoC_{,t-1} + B_{charge,t} - B_{disch,t} \quad (17)$$

where $SoC_{,0}$ (kW) corresponds to the state of charge at the initial time step and $SoC_{,t}$ (kW) refers to the state of charge in the following time steps. In this context two key parameters must be considered—the state of charge (SoC) and the depth of discharge (DoD)—the latter of which refers to the percentage of the battery that has been discharged in comparison to the overall capacity. The initial SoC is set at 50%, aligning with the initial charge level of the storage tank when compared with a PAT system. However, the maximum permissible discharge is 97%, reflecting the use of deep-discharge battery technology while maintaining a small buffer to prevent complete depletion.

3.3. Scenario 3: Parallel Management Using a Centralized Storage Configuration

Scenario 3 introduces a shift in the case study by implementing three modules operating in parallel, each individually assigned to one of the selected consumption profiles. In

this configuration, a single shared storage unit is employed for all three modules (Figure 9). Each module primarily seeks to meet the demand of its corresponding consumption profile, while any surplus energy generated is redirected to the shared storage system. This stored energy can then support modules whose generation is insufficient to fully meet their respective demand profiles.

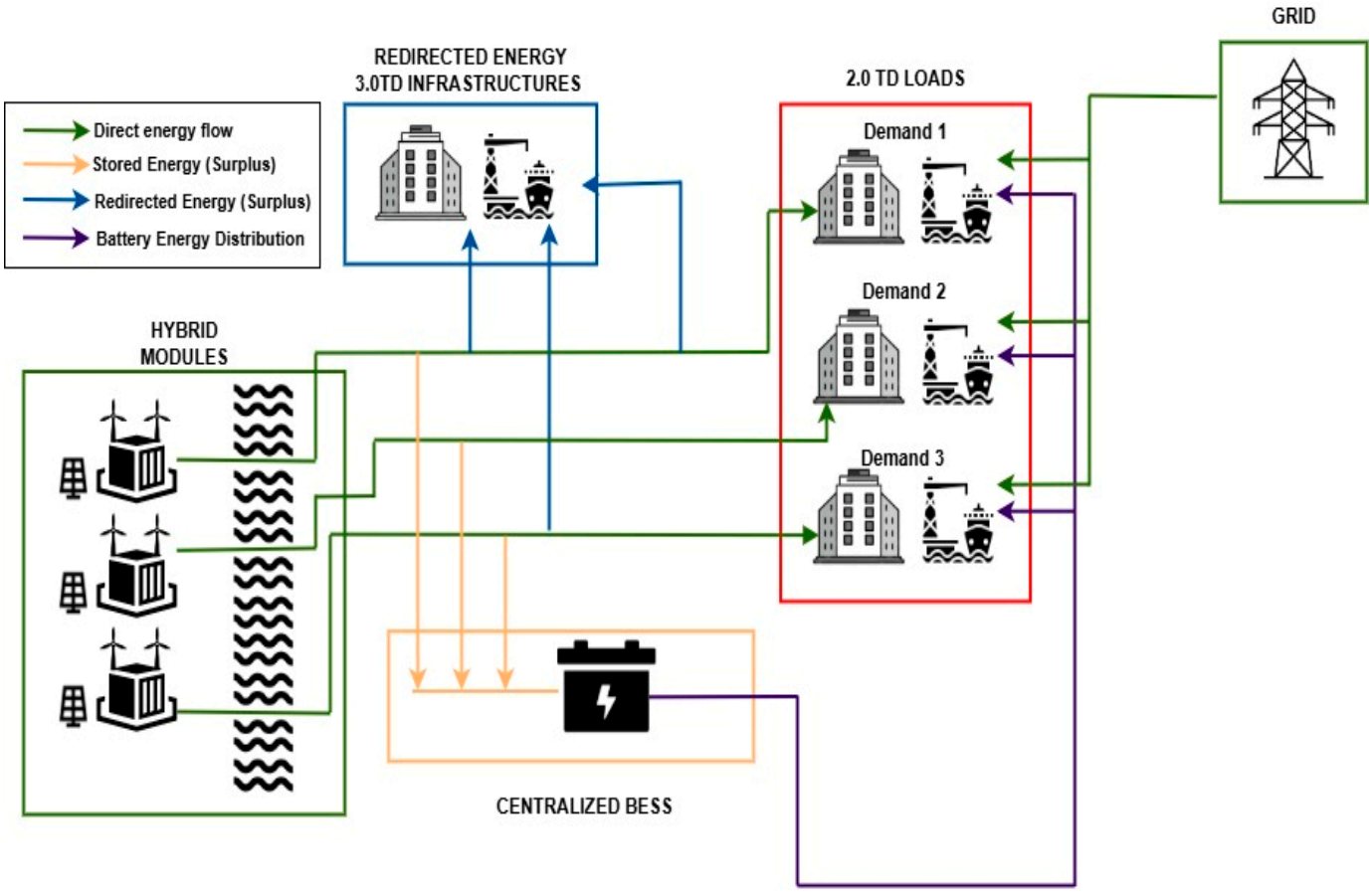

Figure 9. Flow diagram of parallel module distribution with centralized storage unit.

In this case, priority is given to charging the storage system, and once it reaches full capacity, any remaining surplus energy is managed according to the selected excess-energy handling strategy. This represents a slight deviation from the operational approach adopted in the previous two scenarios. The decision to prioritize the storage system at all times makes the use of the PAT system less advantageous, as it exhibits greater inefficiencies compared to battery-based systems and has a lower energy density, thereby limiting the proportion of surplus energy that can be effectively utilized.

The use of three modules instead of a single one means that neither the spatial requirements nor the cost of each module can be maintained as previously defined in the earlier scenarios. The inclusion of additional components, such as containers and higher-cost generation units, for example, wind and hydrokinetic turbines, makes it difficult to implement all three modules within the original budget and spatial constraints, while still allowing flexibility for system optimization through the adjustment of the number of generation units for each source. For this reason, a revised budget limit of 50,000 € is established for this scenario, along with an expanded available area of 200 m^2. It is important to note that not all modules are allocated the same amount of space; rather, the distribution is determined by the assigned consumption profile. Specifically, Module 1 is allocated 120 m^2, Module 2 receives 20 m^2, and Module 3 is assigned 60 m^2. This configuration

enables a more flexible allocation of unit multipliers, aligning generation capacity with the magnitude of each consumption profile. As a result, higher-demand profiles are assigned additional space for components, allowing for increased generation capacity.

The implementation of parallel configurations constitutes a key advancement in this study, enabling a comprehensive evaluation of module performance under coordinated operation. In this arrangement, each module is assigned a unique demand profile, while surplus energy is redirected to a centralized storage system rather than individual storage units. This design strategy aims to maximize resource sharing and inter-module support, thereby enhancing overall system operational synergy.

While the internal logic of the model remains based on the equations established in the initial two scenarios, several dynamic modifications have been introduced. In this configuration, surplus energy generated by any module is consistently directed to support the central storage system rather than being immediately allocated to other modules in need. The central storage then supplies the necessary energy to units unable to meet their assigned demand. This operational approach minimizes deep discharges observed in previous scenarios and prioritizes maintaining support from the generating units to the storage system whenever feasible.

It is important to highlight that this operational approach is advantageous only if the storage system does not introduce significant conversion losses that would reduce overall efficiency. Consequently, batteries represent the most viable option, as the PAT system, with an efficiency of approximately 60%, would incur substantial energy losses when continuously prioritizing storage. Figure 9 illustrates the flow diagram detailing the operation and interactions among the system's primary components.

As previously noted, the fundamental equations governing the system remain largely unchanged; however, minor adjustments have been introduced in the battery loading process. The mentioned modifications are demonstrated in Equations (18)–(20):

$$E_{surplus,t} = \begin{cases} E_{Net(M1),t}, \text{ if } E_{Net(M1),t} > 0 \\ 0, \text{ otherwise} \end{cases} + \begin{cases} E_{Net(M2),t}, E_{Net(M2),t} > 0 \\ 0, \text{ otherwise} \end{cases} + \begin{cases} E_{Net,(M3),t}, E_{Net(M3),t} > 0 \\ 0, \text{ otherwise} \end{cases} \quad (18)$$

$$B_{charge,0} = \begin{cases} E_{surplus,0}, \text{ if } E_{surplus,0} > 0 \text{ and } E_{surplus} + B_{max} \cdot \left(\frac{SoC_{50\%}}{100} \right) \leq B_{max} \\ 0, \text{ if } E_{surplus,0} \leq 0 \\ B_{max} - B_{max} \cdot \left(\frac{SoC_{50\%}}{100} \right), \text{ if } E_{surplus,0} > 0 \text{ and } E_{surplus} + B_{max} \cdot \left(\frac{SoC_{50\%}}{100} \right) \geq B_{max} \end{cases} \quad (19)$$

$$B_{charge,t} = \begin{cases} E_{surplus,t}, \text{ if } SoC_{,t} + E_{surplus,t} \leq B_{max} \\ B_{max} - SoC_{,t}, \text{ if } SoC_{,t} + E_{surplus,t} \geq B_{max} \\ 0, \text{ if } SoC_{,t} = B_{max} \end{cases} \quad (20)$$

where $E_{Net(M1),t}$, $E_{Net(M2),t}$ and $E_{Net(M3),t}$ (kWh) correspond to the net energy balance for module 1, 2 and 3, respectively, at a specific time step, and $E_{surplus,t}$ (kWh) refers to the total combined energy surplus in the parallel management configuration. The rest of the variables have been previously defined.

As presented in Equation (18), the system initially evaluates the energy balance across the three modules, identifying and aggregating any surplus energy. When a positive balance is detected, the system assesses the storage unit's available capacity to absorb this surplus. If sufficient capacity exists, the excess energy is promptly stored in the batteries, without considering potential deficits in other modules. Once the storage system reaches its maximum capacity, any remaining surplus is designated as final surplus and managed according to the predefined strategy, namely, redirecting the energy to other port

infrastructures at preferential rates, as previously outlined. Aside from this adjustment, the system's operational logic remains unchanged, with a distinction made between the initial hour, Equation (19), and the subsequent time periods, Equation (20).

3.4. Scenario 4: Parallel Management Using an Individual Storage Configuration

Scenario 4 presents a different approach from that adopted in Scenario 3, while maintaining the parallel configuration. In this case, the concept of a single centralized storage system for all modules is discarded. Instead, each module is equipped with its own individual storage unit, the capacity of which is optimized according to its specific needs and the established energy coverage parameters. The coverage requirements for each module are defined as follows: Module 1 must achieve more than 75% coverage of its demand through renewable generation and storage, Module 2 more than 95%, and Module 3 more than 90%.

The spatial distribution remains identical to that of Scenario 3. However, rather than applying a shared budget across all modules, this configuration employs an individualized budget of 25,000 € per module. The primary objective of this scenario is to evaluate whether treating each consumption profile independently, without inter-module interactions, can yield improved performance by reducing system dependencies. The use of the PAT system in this scenario is also limited. Since it involves a storage configuration with a larger number of auxiliary components, it requires significantly more space for installation. In contrast, the battery system is integrated directly within the container itself, which also houses the remaining electronic components. As a result, it does not require any additional installation space.

In the final scenario (Figure 10), a decentralized storage configuration is evaluated to assess whether assigning one storage unit per module, rather than relying on a centralized system, can improve overall system performance and better align with the specific demand profiles of each module. In this setup, storage capacity is treated as an independent variable and included in the optimization process to determine the actual capacity required for each module individually. A key characteristic of this configuration is the minimal interaction between modules. Each storage unit is designed to satisfy the respective module's demand constraints autonomously, significantly reducing the need for energy transfer between modules. As in previous scenarios, the available space remains a critical constraint, heavily influencing the choice of storage technology.

The pump-as-turbine system, while technically viable, presents substantial spatial limitations due to the need for auxiliary components, particularly a storage tank, which occupies considerable space. This makes the PAT system less compatible with the modular design constraints. In contrast, battery storage offers a more compact and space-efficient solution. Its smaller dimensions enable integration within the container itself, thereby preserving space for additional generation units. Given these factors, the battery system has been selected as the most suitable technology for this scenario. Nonetheless, for the sake of comparison, the same configuration has also been modeled using the PAT system.

Regarding the internal logic that governs the operation of this strategy, the differences between Scenario 4 and Scenario 2 are minimal. In both cases, the primary objective is to use the generated energy to meet the assigned demand as much as possible. Any surplus energy is then directed to the storage system to provide support during periods of insufficient generation. The storage system of each module is designed exclusively to meet its own energy demand and cannot be used to support other modules. Allowing one module to supply energy to another could jeopardize its ability to cover its future consumption, potentially leading to system inefficiencies or imbalances, depending on the way it is configured.

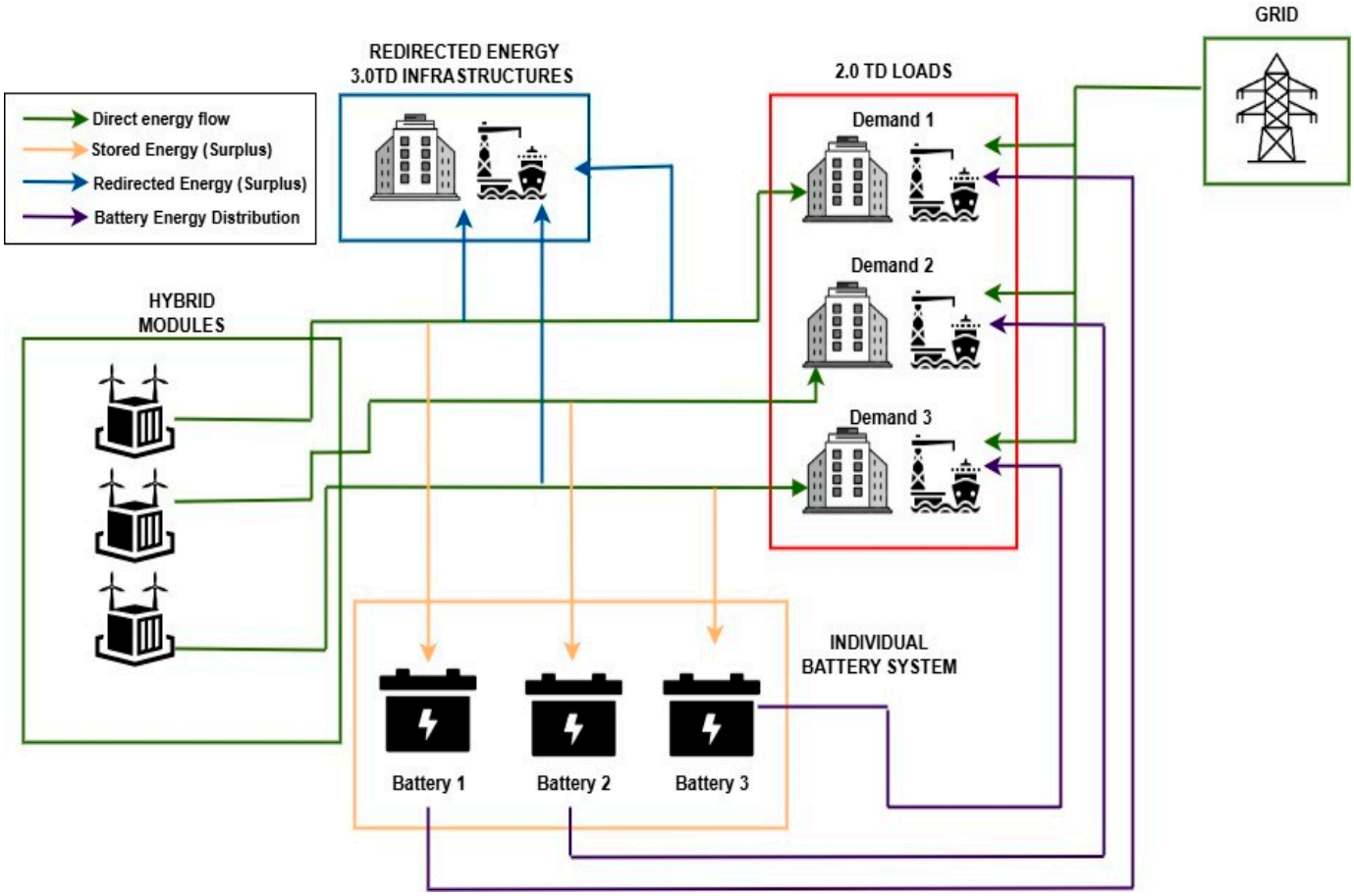

Figure 10. Flow diagram of parallel module distribution with individual storage systems.

The main distinction lies in the allocation of demand: whereas Scenario 2 concentrated all three demand profiles in a single module, the current scenario distributes them across three separate modules. However, the same set of operational equations is applied independently to each module. Due to this new configuration and the relatively low energy demand of some of the selected infrastructures, a significant energy surplus is expected across all modules. As a result, the subsequent redistribution of this excess energy becomes a critical aspect of the system's overall performance. For clarity, Figure 10 presents a flow diagram illustrating the operational logic of this strategy.

4. Results

Based on the scenario descriptions, the results obtained after applying the optimization process are presented, representing the most technically and economically viable configuration for each case.

4.1. Scenarios 1 and 2

The testing of the hybrid module in its original configuration, conducted as a first reference iteration for Scenario 1, did not yield entirely positive results. It was not possible to achieve investment recovery, with parameters such as NPV and IRR showing negative values for both surplus management strategies. Similarly, the target coverage of 70% could not be met, reaching only 58.19%. The application of the optimization process to this configuration resulted in a significant improvement in both energy and economic performance.

The expansion of the photovoltaic unit for Scenario 1, identified as the most cost-effective and space-efficient energy source, from 2 to 38 panels, together with the enlargement of the storage system to 43.36 m^3, enabled renewable sources to achieve a coverage of 60.24%. When combined with an additional 7% contribution from the storage system, the total coverage reached 67.24%, corresponding to 944.38 kWh supplied. All of this was accomplished while remaining within the limits established by the optimization system, with a total cost of the module below 25,000 € (24,521.54 €) and the utilized area staying within the 100 m^2 available (91.5 m^2). With the expansion of the photovoltaic unit, a considerable increase in energy generation was also achieved, rising from 3340.42 kWh to 17,512.55 kWh.

To enable a direct comparison between the two tested storage systems, the results of the first two Scenarios are presented jointly. When considering the optimized version in Scenario 2, which employs batteries as the storage system, the qualitative improvement is substantial. In this case, total demand coverage reaches 89.90%, leaving only 143.33 kWh supplied by the grid. The integration of the batteries within the container itself minimizes the space required for storage, leading to a configuration distinct from that of Scenario 1. Following optimization, the total number of photovoltaic units increases to 42, while the wind unit is expanded to six turbines and the hydrokinetic unit to four. This expansion results in a total surplus of 20,379.02 kWh, representing an additional margin compared to that observed in Scenario 1, which could potentially provide further financial benefits. Figure 11 illustrates the energy performance throughout the year for both scenarios, distinguishing the contributions of each source to provide a clearer visualization of the impact of each unit on the overall system performance.

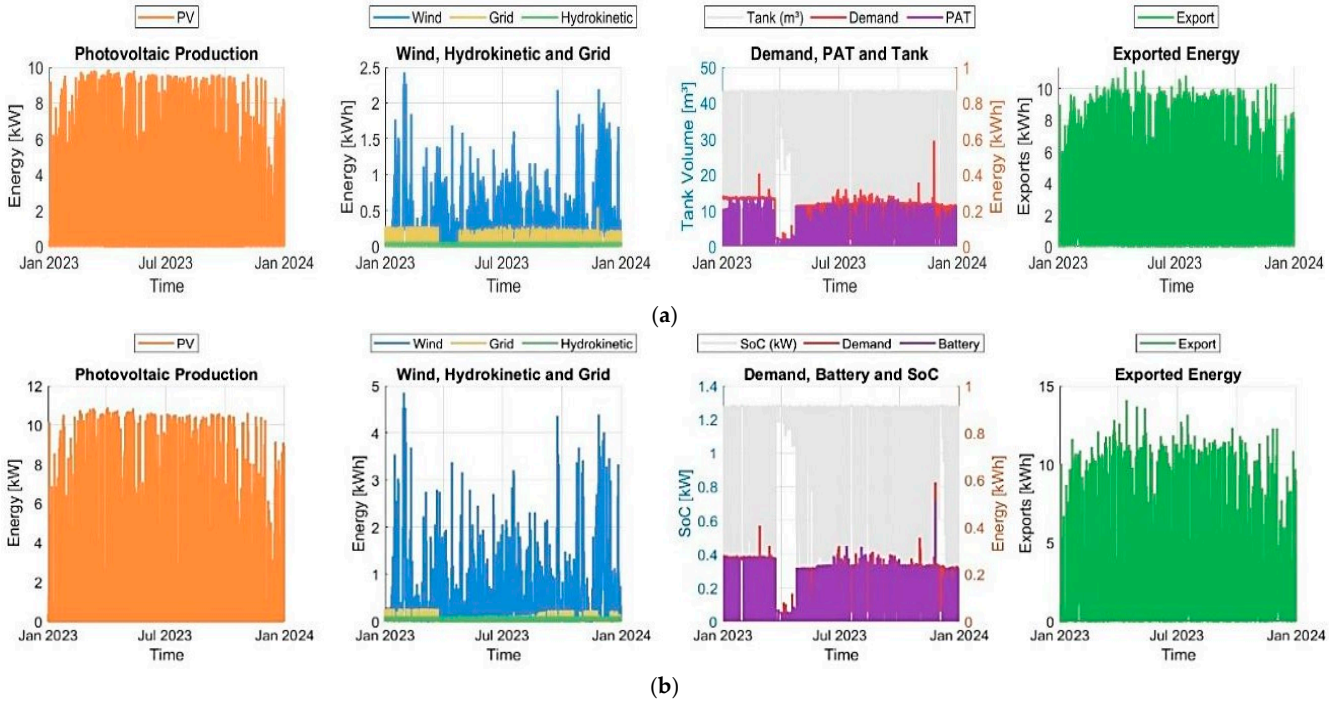

Figure 11. Energy generation and storage performance for Scenario 1 (**a**) and Scenario 2 (**b**).

Regarding the economic aspect, the chosen surplus management strategy has been crucial in achieving positive results and recovering the initial investment. In both scenarios, selling the surplus to the grid did not allow for investment recovery, as the selling prices are lower than the purchase prices. By redirecting the excess energy to other infrastructures, with the 3.0TD tariff assigned, which have higher costs, the investment recovery becomes

significantly faster and more effective. Under this second energy surplus management strategy, the results for both scenarios have demonstrated substantial improvements.

For Scenario 1, the NPV over 25 years, discounted at a 7% interest rate, was 2816.93 €, with an IRR of 8.25% and a payback period of 20 years. Although this option allows for investment recovery, it remains relatively unattractive to investors due to the long payback period and the comparatively low NPV. In Scenario 2, the results were more favorable, owing to higher surplus availability and lower associated costs. Consequently, the NPV for Scenario 2 increased to 9182.79 €, with an IRR of 10.88% and a payback period of 14 years, demonstrating a significant improvement over Scenario 1 (Figure 12). These payback periods may be unattractive for private investors under current market conditions, especially when considering the replacement cycles of battery storage systems. However, battery prices are dropping considerably and the present study is conducted within the framework of the HY4RES research project, which includes laboratory testing, prototype development, and the construction of a NEWLY pilot hybrid module in a port environment, not a fully "optimized and massive" commercial solution.

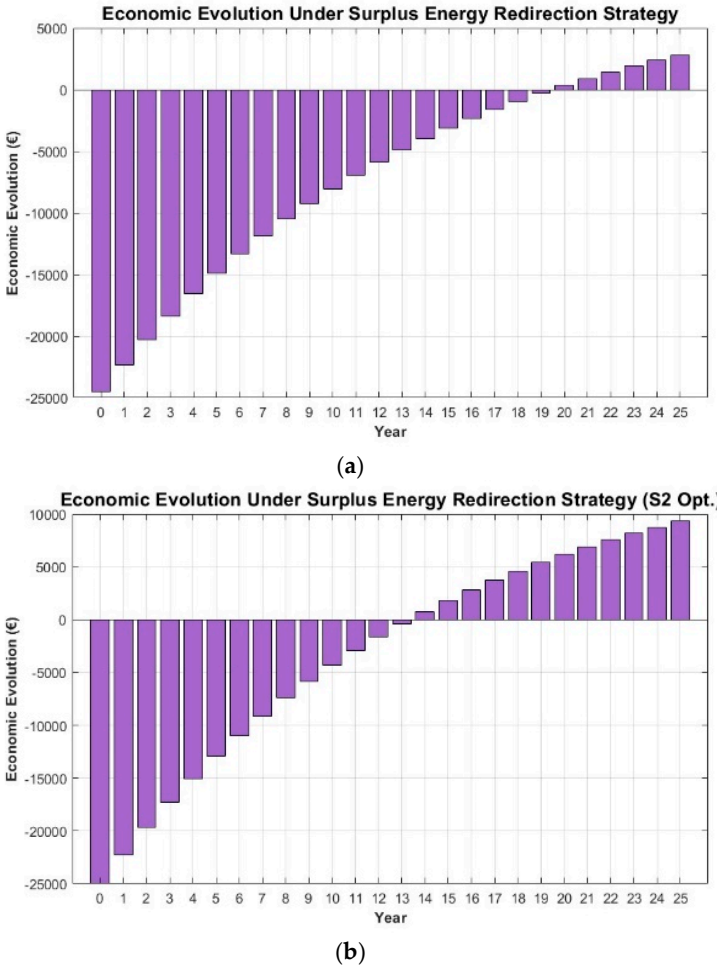

Figure 12. Economic evolution over the 25-year period for Scenario 1 (**a**) and Scenario 2 (**b**).

4.2. Scenarios 3 and 4

Similar to the scenarios with a single module, Scenarios 3 and 4 are analyzed jointly due to their shared parallel structure. It is important to note that these scenarios were only tested with battery storage, as the comparison between Scenario 1 and Scenario 2, especially the results shown in Figure 12, demonstrated a significant financial difference, indicating that feasibility favors the use of batteries.

Starting with Scenario 3, before discussing the energy performance of this configuration in its optimized form, it is important to consider the number of components installed per module. Module 1, after optimization, comprised 64 solar panels, 3 wind turbines, and 2 hydrokinetic turbines. Module 2 maintained its distribution according to the initial design, and Module 3 included 26 solar panels, 3 wind turbines, and 2 hydrokinetic turbines. Regarding storage, given the number of generating units, a single 1 kW battery was sufficient to achieve the desired coverage targets. This configuration entails a final cost of 48,060 €, remaining below the presented limit of 50,000 €, and occupies a total area of 195.34 m^2.

With the system components defined, the energy performance results are presented. This system achieved a final coverage of 90.91% of the total system demand, representing a slight increase of 1.11% compared to Scenario 2. The combined energy surplus from the three modules totals 42,599.97 kWh, which is 109.01% higher than in Scenario 2. These results indicate that near-maximum coverage had already been achieved, so adding more generating units did not further increase demand coverage. In this case, the additional generation provides different benefits, as it allows a larger amount of energy to be redirected to other infrastructures, serving as the primary economic driver for investment recovery (Figure 13).

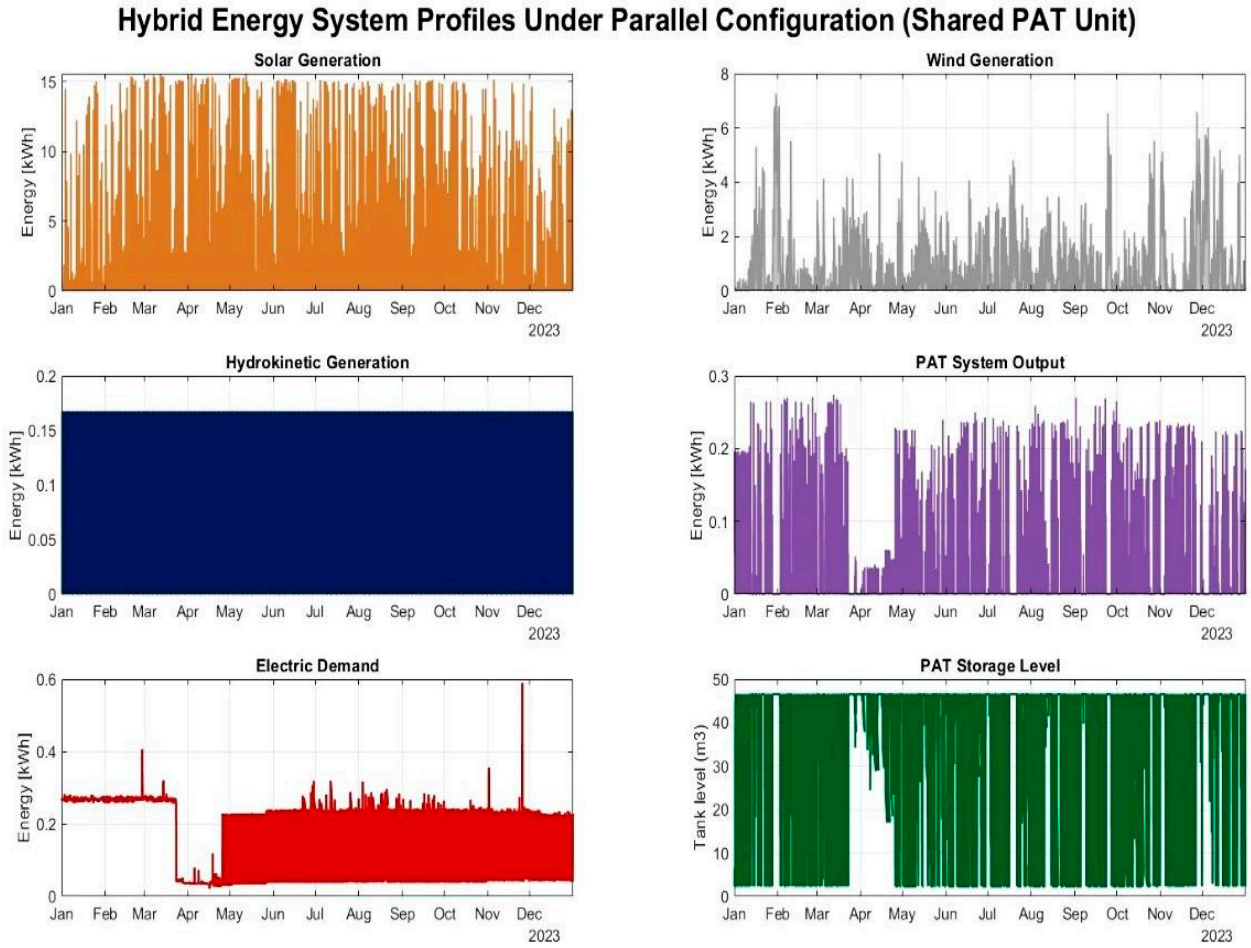

Figure 13. Scenario 3 for energy and storage performance.

In Scenario 4, the results differ notably from the previous configurations, as the reduction in interconnections led to a decline in overall energy efficiency. This scenario comprises 60 solar panels, 3 wind turbines, and 2 hydrokinetic turbines in Module 1, while Modules 2 and 3 retained the same number of installed units as in Scenario 3. A key

distinction in this Scenario is the individualized optimization of storage capacity, which yielded optimal battery sizes of 0.72 kW, 0.01 kW, and 0.07 kW for Modules 1, 2, and 3, respectively. Given the very low demand levels in the latter two modules, the corresponding storage capacities are practically negligible, with values that would be difficult to replicate in real-world market conditions. Nevertheless, these results were retained as part of the optimized configuration.

Under this setup, the total demand coverage achieved in Scenario 4 is considerably lower than that of Scenarios 2 and 3, reaching only 78.48%. Consequently, approximately 302.40 kWh must be imported from the grid to meet the remaining demand. Additionally, the total energy surplus is 1400.17 kWh lower than in Scenario 3. This reduction stems from the individualized budget structure adopted in Scenario 4, which allocates 25,000 € per module rather than a shared budget across all three. As a result, the budget limit for Module 1 was reached, leading to the installation of fewer solar panels than in Scenario 3 and, ultimately, a lower overall energy surplus. In this final scenario, the generation profiles were provided individually for each module. These profiles show that solar generation remains the dominant source, significantly exceeding the contributions from the other technologies. This outcome aligns with the previously observed trend, as the solar component was substantially increased, while the outputs from the wind and hydrokinetic units remained unchanged (Figure 14). The discharge and contribution of the storage system depend strongly on the demand profile and the assigned battery capacity. In particular, Module 1 experiences more frequent discharges reaching the minimum capacity limit compared to Scenario 3, indicating that with higher-demand profiles, the support of the other generating units is essential to mitigate deep discharges.

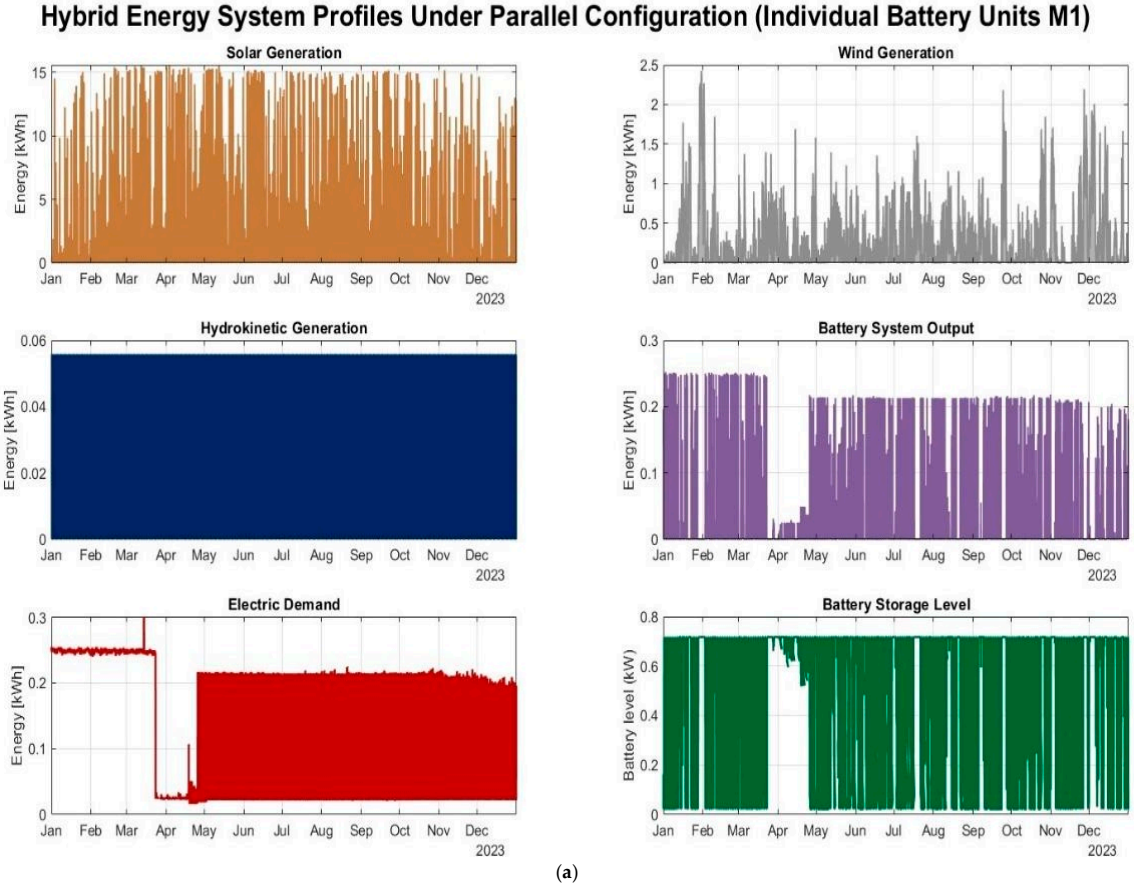

(**a**)

Figure 14. *Cont.*

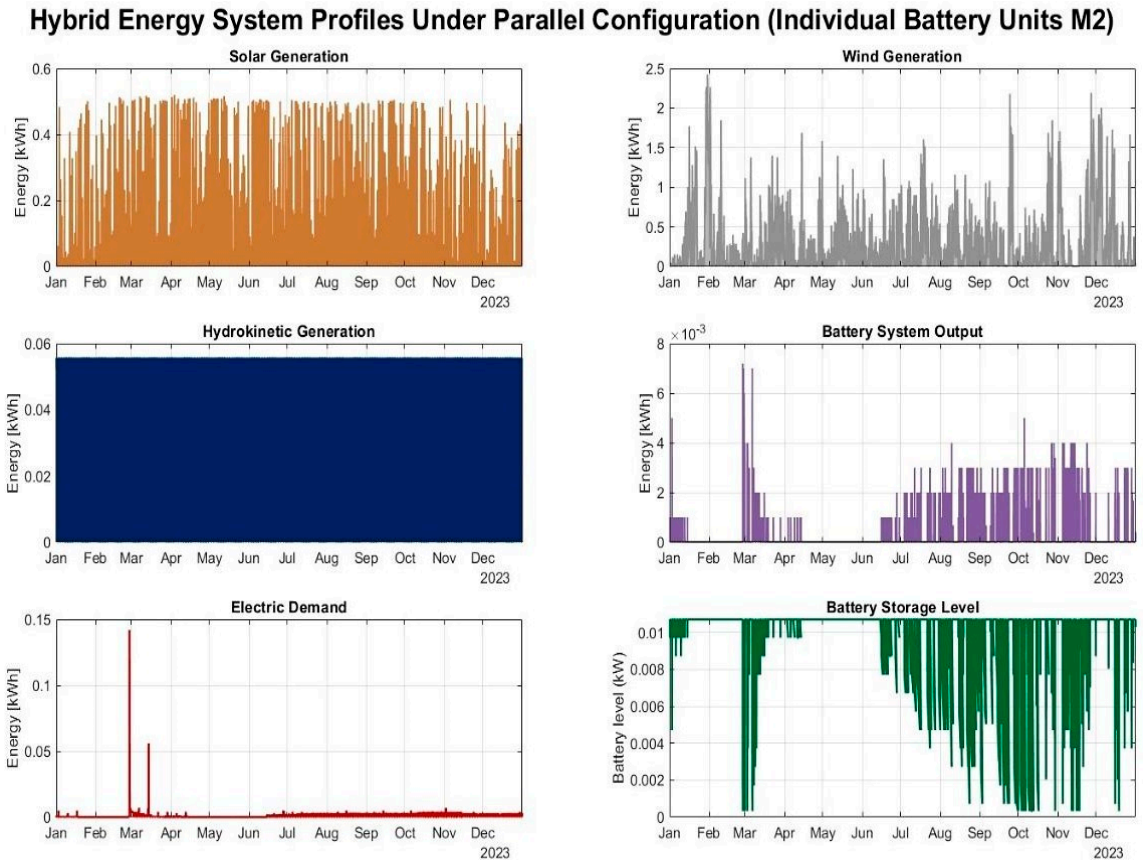

(**b**)

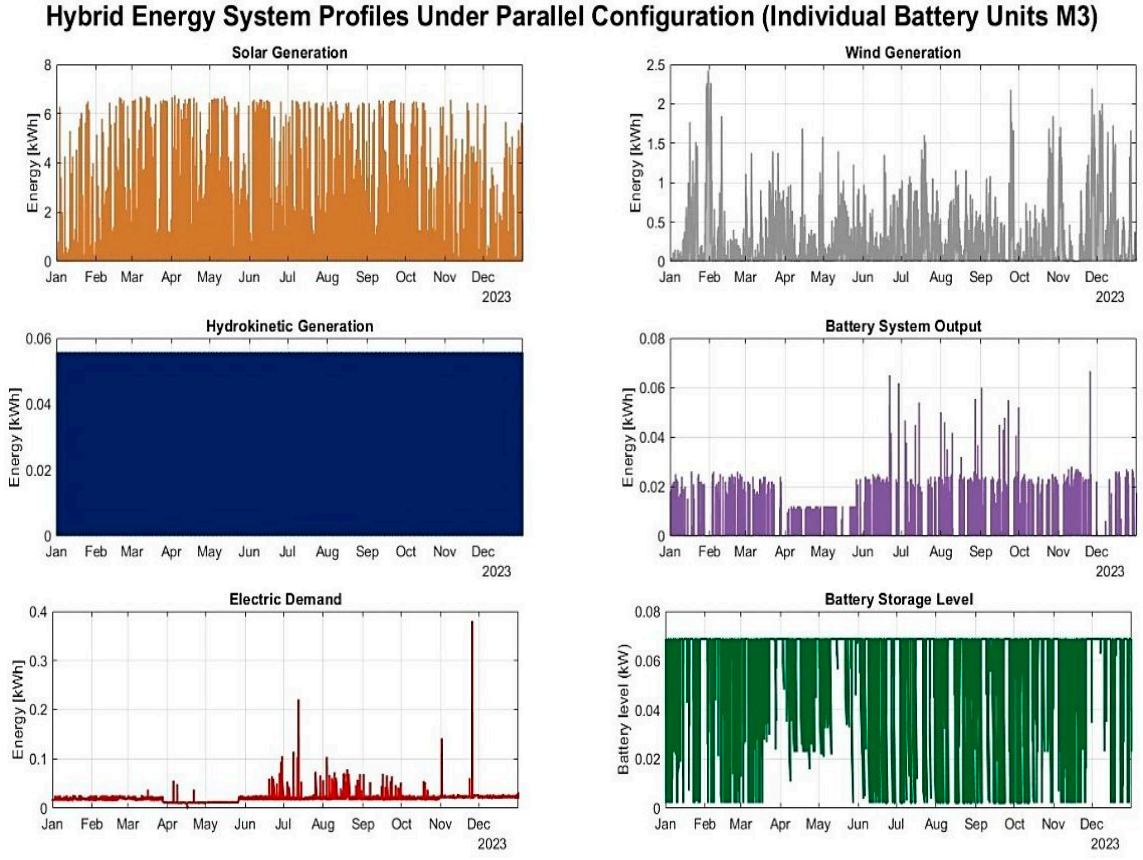

(**c**)

Figure 14. Energy and storage profiles for all three modules in Scenario 4: (**a**) M1; (**b**) M2; (**c**) M3.

Finally, when comparing the financial performance of Scenarios 3 and 4, the results over the 25-year analysis period are remarkably similar. In terms of NPV, the final values, discounted at the same 7% rate used in Scenarios 1 and 2, amount to 21,056.74 € in Scenario 3 and 19,918.45 € in Scenario 4. These results highlight the influence of having a larger and more widely distributed surplus available for redirection to other infrastructures. The corresponding IRRs are 11.54% for Scenario 3 and 11.42% for Scenario 4, both exhibiting a payback period of 13 years (Figure 15).

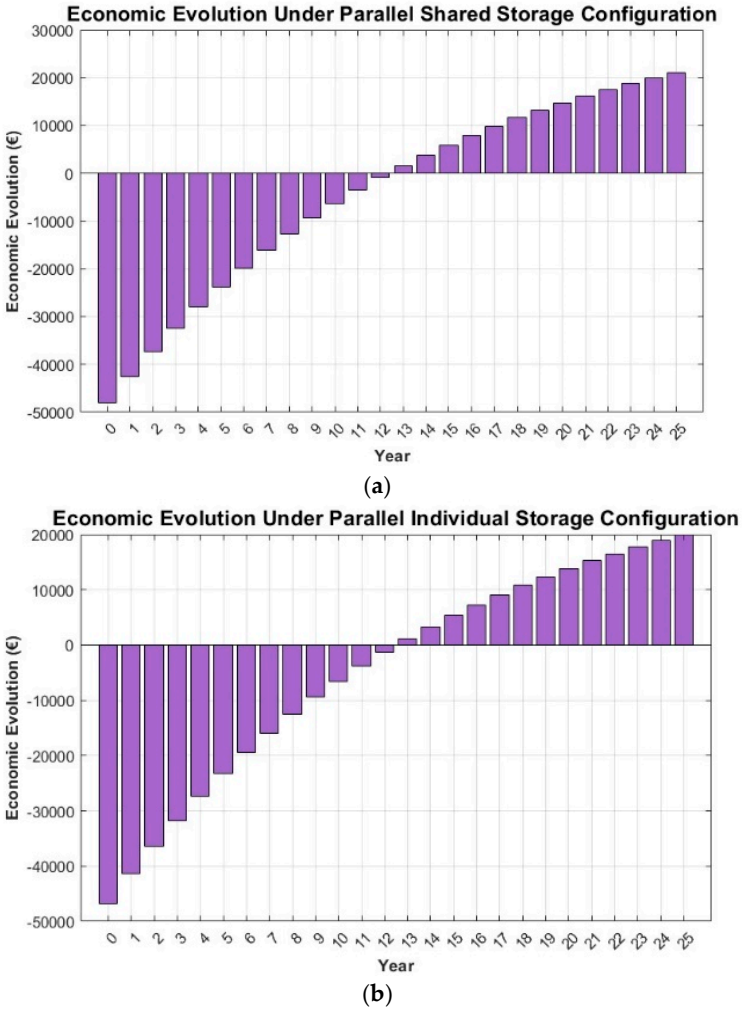

Figure 15. Economic evolution over the 25 years period for Scenario 3 (**a**) and Scenario 4 (**b**).

5. Conclusions

The development of a new Hybrid Operational Strategy (HOPS) model has demonstrated its effectiveness as a structured decision-support tool for optimizing renewable energy integration in port environments. By refining generation values and validating hourly data, the model ensures consistency and reliability in scenario evaluation. The model interface, designed for accessibility and adaptability, enables comprehensive feasibility studies by processing generation profiles, demand patterns, tariff structures, and component costs. Its modular architecture supports up to five generation sources, with current applications focusing on photovoltaic, wind, and hydrokinetic power, complemented by pump-as-turbine or battery storage. The operational logic of HOPS, grounded in energy balance analysis, allows identification of surpluses and deficits, simulation of multiple configurations, and determination of optimal strategies to ensure economic viability. In cases where direct feasibility is not achieved, the tool calculates energy multiplier ratios to

support long-term investment recovery. Migration to Python enhances analytical capabilities, scalability, and integration of advanced storage technologies, positioning HOPS as a versatile platform for sustainable energy planning.

Some relevant key points can be stated as important conclusions:

(i) Development and validation of the HOPS model

This work presents the development of HOPS (Hybrid Operational Strategy), a modular and scalable energy-management and optimization model specifically designed for hybrid renewable systems in port infrastructures. The model successfully integrates photovoltaic, wind, and hydrokinetic generation with two storage technologies (battery and PAT), demonstrating its ability to process real demand profiles, evaluate multiple configurations, and identify the most viable operational strategy.

(ii) Battery storage emerges as the most feasible option

Across all simulated scenarios, battery storage consistently outperformed PAT systems in terms of energy coverage, operational flexibility, and economic feasibility. Under the real demand and generation conditions of the pilot port, the configuration with a single module and battery storage achieved the best performance, supplying 90% of the annual demand and yielding positive economic indicators (NPV = 9182.79 €; IRR = 10.88%).

(iii) Scenario analysis confirms the importance of system configuration

The four scenarios tested—single-module and parallel-module configurations—showed that system architecture significantly affects energy balance and economic outcomes. While parallel operation increases redundancy and potential coverage, it also increases system cost. The results highlight the value of HOPS as a decision-support tool capable of comparing alternative configurations and guiding investment choices.

(iv) Real-world data constraints shape the model's applicability

The study demonstrates that hourly generation and demand data, as provided by the port authority, are sufficient for long-term feasibility assessments. HOPS is designed for steady-state, long-horizon optimization, not for short-term events.

(v) Economic results reflect a research-phase pilot system

The payback periods obtained correspond to a pilot-scale research installation, which includes conception, laboratory testing, prototype development, micro-scale effects, and non-massive production. These values should not be interpreted as commercial benchmarks.

When analyzing the results of the different scenarios, it became evident that increasing generation capacity does not necessarily lead to higher demand coverage, particularly when using renewable generation systems characterized by intermittency. In Scenario 2, a coverage level of 90% was achieved, while in Scenario 3, despite surpluses being 109% higher than in Scenario 2, the coverage only increased by 1.11%. This suggests that, for small self-consumption installations, grouping demands into a single module may be more advantageous than operating them in parallel, as it reduces both space requirements and investment costs. When budget and available space are limited, the use of PAT systems may not be the most optimal storage solution compared with other storage technologies, such as batteries. Another main drawback of PAT systems is their lower efficiency relative to batteries, resulting in reduced coverage and fewer usable surpluses.

Overall, HOPS contributes to advancing efficiency, economic feasibility, and environmental sustainability in hybrid renewable energy systems for ports. Finally, the main avenues for future work include (i) integrating different real operational datasets and other case studies, (ii) expanding the model to incorporate additional technical and socio-economic constraints, and (iii) performing comprehensive different real-world case applications.

Author Contributions: Conceptualization, H.M.R., T.X.A., A.F.J. and R.E.-V.; methodology, H.M.R., T.X.A., O.E.C.-H. and M.P.-S.; software and calculus, T.X.A.; writing—original draft preparation, H.M.R., T.X.A. and A.F.J.; review, M.P.-S., O.E.C.-H., A.M. and R.E.-V.; supervision, H.M.R., M.P.-S., A.M. and R.E.-V.; editing and final preparation, all authors. All authors have read and agreed to the published version of the manuscript.

Funding: This work was supported by FCT, UID/6438/2025 CERIS, in the Hydraulic Laboratory, for experiments on pumped storage performance, and the project HY4RES (Hybrid Solutions for Renewable Energy Systems) EAPA_0001/2022 from INTERREG ATLANTIC AREA PROGRAMME.

Data Availability Statement: The original contributions presented in this study are included in the article. Further inquiries can be directed to the corresponding authors.

Acknowledgments: The authors are grateful for the project HY4RES (Hybrid Solutions for Renewable Energy Systems) EAPA_0001/2022 from the INTERREG ATLANTIC AREA PROGRAMME, as well as the Foundation for Science and Technology's support to UIDB/04625/2025 CERIS for covering the grant of the first author.

Conflicts of Interest: The authors declare no conflicts of interest.

Nomenclature

$B_{charge,0}$	Energy used to charge the battery in the initial time step (kWh)
$B_{charge,t}$	Energy used to charge the battery at a specific time step (kWh)
$B_{disch,0}$	Energy discharged from the battery in the initial time step (kWh)
$B_{disch,t}$	Energy discharged from the battery at a specific time step (kWh)
B_{max}	Battery maximum capacity (kW)
$DoD_{97\%}$	Maximum depth of discharge at 97% of the maximum capacity
$E_{HYDRO,t}$	Energy generated by the Hydro system at a specific time step (kWh)
$E_{LOAD,t}$	Energy demand at a specific time step (kWh)
$E_{NET,0}$	Net energy balance in the initial time step (kWh)
$E_{NET,t}$	Net energy balance at a specific time step (kWh)
$E_{Net(M1),t}$	Net energy balance for module 1 at a specific time step (kWh)
$E_{Net(M2),t}$	Net energy balance for module 2 at a specific time step (kWh)
$E_{Net(M3),t}$	Net energy balance for module 3 at a specific time step (kWh)
$E_{PV,t}$	Energy generated by the PV system at a specific time step (kWh)
$E_{surplus,t}$	Total combined energy surplus in the parallel management (kWh)
$E_{WIND,t}$	Energy generated by the Wind system at a specific time step (kWh)
H	Net head (m)
P	Power output of the wind turbine under operational conditions (W)
P_{max}	Maximum power of the battery that can be discharged in one hour (kW)
P_{turb}	Power output of the wind turbine (W)
$SoC_{50\%}$	State of charge of the battery at 50% of the total capacity (kW)
$SoC_{,0}$	State of charge of the battery in the initial time step (kW)
$SoC_{,t}$	State of charge of the battery at a specific time step (kW)
$SoC_{,t-1}$	State of charge of the battery in the previous time step (kW)
V	Water volume assigned to the PAT system (m^3)
$V_{5\%}$	Volume of water equivalent to 5% of the total storage capacity (m^3)
$V_{50\%}$	Volume of water equivalent to 50% of the total storage capacity (m^3)
$V_{disch,0}$	Volume of water to be discharged in the initial time step (m^3)
$V_{disch,t}$	Volume of water to be discharged at a specific time step (m^3)
$V_{fill,0}$	Volume of water assigned to fill the tank in the initial time step (m^3)
$V_{fill,t}$	Volume of water assigned to fill the tank at a specific time step (m^3)
V_{max}	Maximum storage volume of the tank (m^3)
$V_{need,0}$	Volume needs to satisfy the energy deficit in the initial time step (m^3)
$V_{need,t}$	Volume needs to satisfy the energy deficit at a specific time step (m^3)

$V_{rem,0}$	Remaining volume in the tank in the initial time step (m^3)
$V_{rem,t}$	Remaining volume in the tank at a specific time step (m^3)
$V_{rem,t-1}$	Remaining volume in the tank in the previous time step (m^3)
v	Wind velocity (m/s)
g	Gravitational acceleration (m/s^2)
η_{PAT}	PAT system efficiency
ρ	Water density (kg/m^3)

References

1. Wan, Z.; Nie, A.; Chen, J.; Pang, C.; Zhou, Y. Transforming ports for a low-carbon future: Innovations, challenges, and opportunities. *Ocean. Coast. Manag.* **2025**, *264*, 107636. [CrossRef]
2. European Commission. Decarbonising Maritime Transport—FuelEU Maritime. Mobility and Transport. 2023. Available online: https://transport.ec.europa.eu/transport-modes/maritime/decarbonising-maritime-transport-fueleu-maritime_en (accessed on 1 May 2025).
3. Sustainable Ships. 2025. Available online: https://www.sustainable-ships.org/stories/2025/eu-shore-power-demand-2030 (accessed on 1 May 2025).
4. Hy4res. Port Pilot Site—Port of Aviles—Spain—HY4RES. 2025. Available online: https://hy4res.eu/pilot-sites/port/ (accessed on 20 October 2025).
5. Buonomano, A.; Giuzio, G.F.; Maka, R.; Palombo, A.; Russo, G. Empowering sea ports with renewable energy under the enabling framework of the energy communities. *Energy Convers. Manag.* **2024**, *314*, 118693. [CrossRef]
6. Peng, S.-T.; Qi, Z.-Y.; Liu, Y.-Y.; Liu, Z.-F.; Li, L.-L. Improving the energy efficiency and economic benefits of port integrated energy systems: A multi-objective optimization model for wind-storage-charging-discharging power stations with green efficiency factors-driven multilateral response strategy. *Energy* **2025**, *339*, 138939. [CrossRef]
7. Elsayed, I.; Kanaan, H.; Mehanna, M. Feasibility and optimal sizing analysis of hybrid PV/Wind powered seawater desalination system: A case study of four locations, Egypt. *Heliyon* **2024**, *10*, e40313. [CrossRef]
8. Tang, D.; Zheng, Z.; Guerrero, J.M. A hybrid multi-criteria dynamic sustainability assessment framework for integrated multi-energy systems incorporating hydrogen at ports. *Int. J. Hydrogen Energy* **2024**, *99*, 540–552. [CrossRef]
9. Micallef, A.; Apap, M.; Licari, J.; Spiteri Staines, C.; Xiao, Z. Renewable energy systems in offshore platforms for sustainable maritime operations. *Ocean Eng.* **2025**, *319*, 120209. [CrossRef]
10. Elalfy, D.A.; Gouda, E.; Kotb, M.F.; Bureš, V.; Sedhom, B.E. Comprehensive review of energy storage systems technologies, objectives, challenges, and future trends. *Energy Strategy Rev.* **2024**, *54*, 101482. [CrossRef]
11. Koholé, Y.W.; Wankouo Ngouleu, C.A.; Fohagui, F.C.V.; Tchuen, G. A comprehensive comparison of battery, hydrogen, pumped-hydro and thermal energy storage technologies for hybrid renewable energy systems integration. *J. Energy Storage* **2024**, *93*, 112299. [CrossRef]
12. Pare, S. Walvis Bay Saltworks: The Monster Refinery in Namibia with Colorful Ponds that Cover the Land Like Patchwork. Live Science. 2025. Available online: https://www.livescience.com/planet-earth/walvis-bay-saltworks-the-monster-refinery-in-namibia-with-colorful-ponds-that-cover-the-land-like-patchwork?utm_source (accessed on 8 July 2025).
13. Khalili, Y.; Yasemi, S.; Bagheri, M.; Sanati, A. Advancements in hydrogen storage technologies: Integrating with renewable energy and innovative solutions for a sustainable future. *Energy Geosci.* **2025**, *6*, 100408. [CrossRef]
14. Cholidis, D.; Sifakis, N.; Savvakis, N.; Tsinarakis, G.; Kartalidis, A.; Arampatzis, G. Enhancing Port Energy Autonomy Through Hybrid Renewables and Optimized Energy Storage Management. *Energies* **2025**, *18*, 1941. [CrossRef]
15. Zheng, Y.; Zhou, X.; Yu, J.; Xue, X.; Wang, X.; Tu, X. Predictive analytics for sustainable energy: An in-depth assessment of novel Stacking Regressor model in the off-grid hybrid renewable energy systems. *Energy* **2025**, *324*, 135916. [CrossRef]
16. Tahir, K.A. A Systematic Review and Evolutionary Analysis of the Optimization Techniques and Software Tools in Hybrid Microgrid Systems. *Energies* **2025**, *18*, 1770. [CrossRef]
17. Teng, F.; Zhang, Q.; Xiao, G.; Ban, Z.; Liang, Y.; Guan, Y. Energy Management for a Port Integrated Energy System Based on Distributed Dual Decomposition Mixed Integer Linear Programming. *J. Mar. Sci. Eng.* **2023**, *11*, 1137. [CrossRef]
18. Kim, S.; Heo, S.; Nam, K.; Woo, T.; Yoo, C. Flexible renewable energy planning based on multi-step forecasting of interregional electricity supply and demand: Graph-enhanced AI approach. *Energy* **2023**, *282*, 128858. [CrossRef]
19. Hwang, J.; Yoon, S. AI agent-based indoor environmental informatics: Concept, methodology, and case study. *Build. Environ.* **2025**, *277*, 112879. [CrossRef]
20. Sifakis, N.; Konidakis, S.; Tsoutsos, T. Hybrid renewable energy system optimum design and smart dispatch for nearly Zero Energy Ports. *J. Clean. Prod.* **2021**, *310*, 127397. [CrossRef]

21. Maghami, M.R.; Mutambara, A.G.O. Challenges associated with Hybrid Energy Systems: An artificial intelligence solution. *Energy Rep.* **2023**, *9*, 924–940. [CrossRef]
22. Tawfik, M.; Shehata, A.S.; Hassan, A.A.; Kotb, M.A. Renewable solar and wind energies on buildings for green ports in Egypt. *Environ. Sci. Pollut. Res.* **2023**, *30*, 47602–47629. [CrossRef]
23. Hwang, J.; Kim, J.; Yoon, S. DT-BEMS: Digital twin-enabled building energy management system for information fusion and energy efficiency. *Energy* **2025**, *326*, 136162. [CrossRef]
24. Fernández-Jiménez, A. *HY4RES Project Report: Pilot Site Mapping (Port of Avilés)*; Version 2; University of Oviedo (UNIOVI): Oviedo, Spain, 2024.
25. European Commission. Photovoltaic Geographical Information System (PVGIS). 2025. Available online: https://joint-research-centre.ec.europa.eu/photovoltaic-geographical-information-system-pvgis_en (accessed on 1 May 2025).
26. Puertos del Estado. PORTUS (Puertos del Estado). 2024. Available online: https://portus.puertos.es/#/ (accessed on 1 June 2025).
27. Cholidis, D.; Sifakis, N.; Chachalis, A.; Savvakis, N.; Arampatzis, G. Energy Transition Framework for Nearly Zero-Energy Ports: HRES Planning, Storage Integration, and Implementation Roadmap. *Sustainability* **2025**, *17*, 5971. [CrossRef]
28. Ramos, H.M.; Coelho, J.S.T.; Bekci, E.; Adrover, T.X.; Coronado-Hernández, O.E.; Perez-Sanchez, M.; Koca, K.; McNabola, A.; Espina-Valdés, R. Optimization and Machine Learning in Modeling Approaches to Hybrid Energy Balance to Improve Ports' Efficiency. *Appl. Sci.* **2025**, *15*, 5211. [CrossRef]
29. Nasir, A.; Dribssa, E.; Girma, M.; Madessa, H.B. Selection and Performance Prediction of a Pump as a Turbine for Power Generation Applications. *Energies* **2023**, *16*, 5036. [CrossRef]